© 2014. Published by The Company of Biologists Ltd | Journal of Cell Science (2014) 127, 259 doi:10.1242/jcs.146225

CORRECTION

Fission yeast nucleolar protein Dnt1 regulates G2/M transition and cytokinesis by downregulating Wee1 kinase

Zhi-yong Yu, Meng-ting Zhang, Gao-yuan Wang, Dan Xu, Daniel Keifenheim, Alejandro Franco, Jose Cansado, Hirohisa Masuda, Nick Rhind, Yamei Wang and Quan-wen Jin

There was an error published in *J. Cell Sci.* **126**, 4995-5004.

One source of funding was accidentally omitted. The correct funding section is as shown below.

Funding

This work was supported by the National Institutes of Health [grant number GM-069957 to N.R.]; MEC European Regional Development Fund co-funding from the EU [grant number BFU2011-22517 to J.C.]; the National Natural Science Foundation of China [grant number 31171298 to Q.W.J.]; Key Project of the Chinese Ministry of Education [grant number 108076 to Q.W.J.]; the 111 Project of Education of China [grant number B06016]. H.M. is supported by Cancer Research UK (grant to Takashi Toda, Laboratory of Cell Regulation, Cancer Research UK London Research Institute, Lincoln's Inn Fields, London, UK). Deposited in PMC for release after 12 months.

We apologise to the readers for this error.

Fission yeast nucleolar protein Dnt1 regulates G2/M transition and cytokinesis by downregulating Wee1 kinase

Zhi-yong Yu[1], Meng-ting Zhang[1], Gao-yuan Wang[1], Dan Xu[1], Daniel Keifenheim[2], Alejandro Franco[3], Jose Cansado[3], Hirohisa Masuda[4], Nick Rhind[2], Yamei Wang[1,*] and Quan-wen Jin[1,*]

[1]State Key Laboratory of Cellular Stress Biology, School of Life Sciences, Xiamen University, Xiamen 361102, Fujian, China
[2]Department of Biochemistry and Molecular Pharmacology, University of Massachusetts Medical School, 364 Plantation St., Worcester, MA 01605, USA
[3]The Yeast Physiology Group, Department of Genetics and Microbiology, Facultad de Biología, Universidad de Murcia, 30071 Murcia, Spain
[4]Laboratory of Cell Regulation, Cancer Research UK London Research Institute, Lincoln's Inn Fields Laboratories, 44 Lincoln's Inn Fields, London WC2A 3LY, UK

*Authors for correspondence (wangyamei@xmu.edu.cn; jinquanwen@xmu.edu.cn)

Accepted 5 August 2013
Journal of Cell Science 126, 4995–5004

doi: 10.1242/jcs.132845

Summary

Cytokinesis involves temporally and spatially coordinated action of the cell cycle, cytoskeletal and membrane systems to achieve separation of daughter cells. The septation initiation network (SIN) and mitotic exit network (MEN) signaling pathways regulate cytokinesis and mitotic exit in the yeasts *Schizosaccharomyces pombe* and *Saccharomyces cerevisiae*, respectively. Previously, we have shown that in fission yeast, the nucleolar protein Dnt1 negatively regulates the SIN pathway in a manner that is independent of the Cdc14-family phosphatase Clp1/Flp1, but how Dnt1 modulates this pathway has remained elusive. By contrast, it is clear that its budding yeast relative, Net1/Cfi1, regulates the homologous MEN signaling pathway by sequestering Cdc14 phosphatase in the nucleolus before mitotic exit. In this study, we show that *dnt1*$^{+}$ positively regulates G2/M transition during the cell cycle. By conducting epistasis analyses to measure cell length at septation in double mutant (for *dnt1* and genes involved in G2/M control) cells, we found a link between *dnt1*$^{+}$ and *wee1*$^{+}$. Furthermore, we showed that elevated protein levels of the mitotic inhibitor Wee1 kinase and the corresponding attenuation in Cdk1 activity is responsible for the rescuing effect of *dnt1Δ* on SIN mutants. Finally, our data also suggest that Dnt1 modulates Wee1 activity in parallel with SCF-mediated Wee1 degradation. Therefore, this study reveals an unexpected missing link between the nucleolar protein Dnt1 and the SIN signaling pathway, which is mediated by the Cdk1 regulator Wee1 kinase. Our findings also define a novel mode of regulation of Wee1 and Cdk1, which is important for integration of the signals controlling the SIN pathway in fission yeast.

Key words: Fission yeast, Nucleolus, Dnt1, Wee1, G2/M transition, Cytokinesis

Introduction

Eukaryotic cells use a highly conserved mechanism to control entry into mitosis, which depends on the activation of cyclin-dependent kinase (CDK), a key enzyme consisting of the protein kinase Cdk1 and its regulatory subunit, cyclin B (Morgan, 1997; Nurse, 1990). The highly activated Cdk1 drives entry into mitosis by phosphorylating a wide range of targets (Lindqvist et al., 2009; Ubersax et al., 2003). In the fission yeast *Schizosaccharomyces pombe*, the machinery regulating entry into mitosis has been thoroughly characterized (Nurse, 1994). The activity of the fission yeast Cdk1 (encoded by the *cdc2*$^{+}$ gene) oscillates throughout the cell cycle, peaking as cells enter mitosis (Morgan, 1997). During interphase, Cdk1 activity is held in check by the inhibitory phosphorylation on conserved tyrosine 15 (Tyr^{15}) in the ATP binding domain by Mik1 and Wee1 kinases (Berry and Gould, 1996; Lundgren et al., 1991; Russell and Nurse, 1987b), and this modification interferes with the ability of Cdk1 to transfer phosphate to the target substrate (Morgan, 1997). Upon the G2/M transition and mitotic onset, a sharp reversal of this phosphorylation event is triggered by the Cdc25 family of phosphatases, which act as a major rate-limiting step in the activation of Cdk1 (Millar et al., 1991; Nilsson and Hoffmann, 2000; Russell and Nurse, 1986).

Both Wee1 kinase and Cdc25 phosphatase are in turn tightly regulated to provide an accurate control of the mitotic onset, and a variety of factors and signaling pathways converge upon Wee1 and Cdc25 to govern the G2/M transition (Callegari and Kelly, 2007; Calonge et al., 2010; Kuntz and O'Connell, 2009; López-Avilés et al., 2005; O'Connell et al., 2000; Suda et al., 2000). Among them, the MAP-kinase-mediated stress-nutritional response (SR), the cell-geometry sensing (CGS) and the G2 DNA-damage-checkpoint pathways, all regulate Tyr^{15} phosphorylation through Wee1 and Cdc25 (Callegari and Kelly, 2007; Martin and Berthelot-Grosjean, 2009; Millar et al., 1995; Moseley et al., 2009; Petersen and Nurse, 2007; Rhind et al., 1997; Russell and Nurse, 1987a; Shiozaki et al., 1998). The SR pathway connects the nutrient-responding TOR pathway with the recruitment of Polo kinase (Plo1) to the spindle pole body (SPB)

and Cdk1 activation, and is responsible for nutritional modulation of mitotic entry (Petersen and Hagan, 2005; Petersen and Nurse, 2007). The CGS pathway controls mitotic entry in response to cell geometry through two related inhibitory kinases of Wee1, Cdr1/Nim1 and Cdr2, and it involves a spatial gradient of the protein kinase Pom1 along the long axis of the cell, coupling cell length to G2/M transition (Hachet et al., 2011; Martin and Berthelot-Grosjean, 2009; Moseley et al., 2009). Finally, the G2 DNA damage delays entry into mitosis primarily by inhibiting Cdc25, but it also has a secondary effect through the activation of Mik1 (Rhind et al., 1997; Rhind and Russell, 2001).

Wee1 has been shown to be destabilized during G2 and M phases of the cell cycle in diverse organisms ranging from yeasts to humans, and therefore degradation is thought to be a major mechanism triggering the decrease in Wee1 levels as cells enter mitosis (Aligue et al., 1997; Kellogg, 2003; McGowan and Russell, 1995; Sia et al., 1998; Watanabe et al., 2005). It has been demonstrated that a multicomponent E3 (ubiquitin ligase), the SCF (Skp1–Cdc53/Cullin-1–F-box) complex, is responsible for Wee1 degradation at the onset of M-phase in budding yeast, frog egg extracts and human somatic cells (Kaiser et al., 1998; Michael and Newport, 1998; Watanabe et al., 2004). However, whether SCF-mediated Wee1 degradation is conserved in fission yeast awaits direct evidence, although it has been shown that *skp1* mutants display cell elongation and G2-delay phenotypes (Lehmann et al., 2004).

In fission yeast, a spindle pole body (SPB)-based regulatory network, called the septation initiation network (SIN), triggers exit from mitosis and cytokinesis. The SIN is homologous to the mitotic exit network (MEN) in budding yeast, although the two pathways have diverged in function (reviewed by Balasubramanian et al., 2004; Gould and Simanis, 1997; Guertin et al., 2002a; Krapp and Simanis, 2008). The SIN signaling cascade is initiated by activation of the GTPase Spg1 and promoted by three protein kinases and their associated subunits: Cdc7, Sid1-Cdc14 and Sid2-Mob1. Assembly of SIN signaling components and their regulators occurs at the SPB on a platform built by the SIN scaffolding components Cdc11 and Sid4, which recruit all the members of the SIN to the SPBs. The SIN controls the final stages of cell division, including actomyosin ring contraction and formation of the division septum. Loss-of-function mutations in *sin* genes result in elongated multinucleate cells as a result of multiple rounds of nuclear division, and cell growth in the absence of cell division.

SIN signaling needs to coordinate cytokinesis with completion of chromosome segregation and is negatively regulated by Cdk1 activity. Previous studies have shown that the transition from a symmetrical to an asymmetrical distribution of Cdc7 kinase on the SPBs during anaphase, the initial association of Sid1 kinase with only the new SPB at anaphase B, and maximum SIN activation, are all dependent upon Cdk1 inhibition (Chang et al., 2001; Dischinger et al., 2008; Guertin et al., 2000).

Previously, in a genetic screen for suppressors of the cytokinesis checkpoint defect in SIN mutants, we identified the nucleolar protein Dnt1 as an inhibitor of SIN signaling (Jin et al., 2007). Although the amino acid sequence of Dnt1 shows weak similarity to that of budding yeast nucleolar proteins Net1/Cfi1, it seems that Dnt1 functions in a distinct way from Net1/Cfi1. Our study revealed that, unlike Net1/Cfi1, which regulates the MEN through the Cdc14 phosphatase, Dnt1 inhibits the SIN independently of Clp1/Flp1 (hereafter referred to as Clp1), the fission yeast homologue of Cdc14 (Jin et al., 2007). However, a detailed mechanism explaining how Dnt1 antagonizes the SIN signaling in fission yeast remained unclear.

In this work, we show that *S. pombe* cells display a delay in G2/M transition during the cell cycle in the absence of *dnt1*$^+$, and this delay correlated with persistent Tyr^{15} phosphorylation on Cdk1. Genetic and biochemical analyses revealed that the G2/M transition defect in *dnt1Δ* cells is due to elevated activity and protein level of the mitotic inhibitor Wee1 kinase, because removal of Wee1 completely abolished the rescuing effect of *dnt1Δ* on SIN mutants. Finally, our data also suggest that Dnt1 modulates Wee1 activity in parallel with SCF-mediated Wee1 degradation. Thus, in fission yeast Dnt1 negatively regulates SIN signaling by modulating the protein levels of Wee1 and therefore the activity of Cdk1. The above findings reveal the existence of a novel mode of control of SIN by a nucleolar protein.

Results

Dnt1 positively regulates G2/M transition in the cell cycle

While studying *dnt1*$^+$ for its role in cytokinesis, we made several observations that indicate that *dnt1*$^+$ might also regulate the cell cycle progression. First, the rescuing effect of *dnt1Δ* on temperature-sensitive SIN mutants *cdc14-118*, *sid2-250* and actomyosin ring formation mutant *cdc8-110* was sensitive to protein level or activity of Cdc25, because the enhanced growth at 30℃ or 33℃ of double mutants *dnt1Δ cdc14-118*, *dnt1Δ sid2-25* and *dnt1Δ cdc8-110* compared with single mutants *cdc14-118*, *sid2-250* or *cdc8-110*, was abolished when higher levels of Cdc25 were induced by a gain-of-function version of *cdc25*$^+$ (i.e. *nmt1-cdc25-D1*) (Daga and Jimenez, 1999; Tallada et al., 2007) (Fig. 1A and supplementary material Fig. S1). Second, *dnt1Δ* deletion was synthetically sick with the temperature-sensitive mutant of *cdc25-22* (Fig. 1B). Third, *dnt1Δ* deletion was synthetic lethal with *cdc25Δ* in a *cdc2-3w* genetic background, which is largely insensitive to Cdc25 (Fantes, 1981). When *cdc2-3w cdc25Δ::ura4*$^+$ cells were crossed with the *dnt1Δ::kan*^{R} *cdc2-3w* mutant, triple mutant spores germinated to form microcolonies with elongated branched cells that stopped dividing after several cell divisions (Fig. 1C). Fourth, we also noticed that *dnt1Δ* cells divided at a significantly longer length than wild-type cells, and this was also true for *cdc25-22 dnt1Δ* cells when compared with *cdc25-22* cells (Fig. 1D,E). In *S. pombe*, there is a direct correlation between cell length at septation and the timing of mitotic commitment, and a longer cell length at division indicates mitotic delay (Mitchison and Nurse, 1985). Thus, the above data suggest that Dnt1 might be a Cdc25-independent positive regulator of G2/M transition in fission yeast.

Next, we examined whether levels of Cdc2 itself and its phosphorylation at Tyr^{15} (pY15) were affected by the absence of *dnt1*$^+$. We found that whereas Cdc2 protein level remained unchanged in *dnt1Δ* cells, Cdc2 phosphorylation at Tyr^{15} was significantly increased in these cells (Fig. 2A,B). To more directly monitor the levels of Cdc2 phosphorylation at Tyr^{15} during the cell cycle, we performed a *cdc25-22* block-and-release assay. Cells synchronized in G2 by the temperature-sensitive *cdc25-22* mutation were released to permissive temperature to allow mitotic entry. As shown in Fig. 2C, the kinetics of Cdc2 dephosphorylation at Tyr^{15} in *cdc25-22 dnt1Δ* cells was notably delayed compared with control cells. The maximum percentage of binucleated (entering mitosis) and septated cells was also reduced for an extended period in the *cdc25-22 dnt1Δ* mutant, confirming a cell cycle defect at G2. Moreover, the duration of

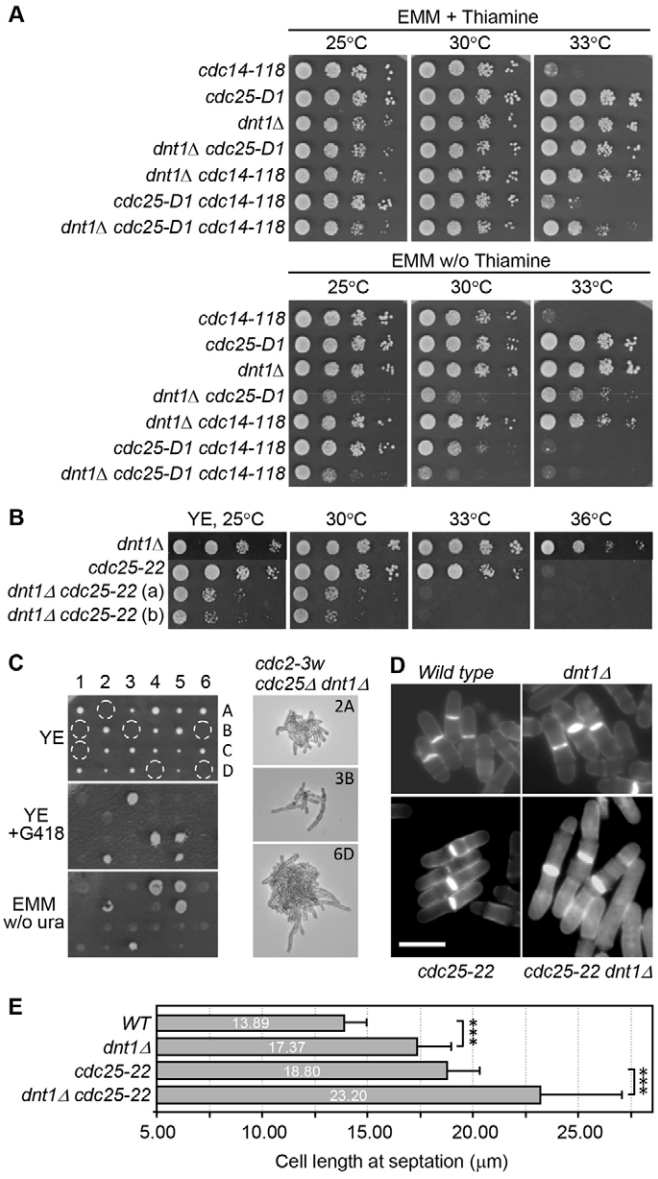

Fig. 1. Characterization of cell-cycle-progression defects in *dnt1Δ* cells. (A) The suppressive effect of *dnt1Δ* on the temperature-sensitive SIN mutant *cdc14-118* is counteracted by increased levels of Cdc25 in a gain-of-function version of *cdc25*$^{+}$ (*nmt1-cdc25-D1*). Serial dilutions (10-fold) of the indicated strains were spotted on EMM with or without thiamine and incubated at the indicated temperatures. (B) Negative genetic interaction between *dnt1Δ* and *cdc25-22*. Serial dilutions (10-fold) of the indicated strains were spotted on YE plates and incubated for 3–5 days at the indicated temperatures before being photographed. (C) *dnt1Δ* deletion is synthetic lethal with *cdc25Δ* in a *cdc2-3w* genetic background. Normal-looking four-spore asci obtained on sporulating ME plates for 2 days after a cross between *dnt1Δ::kan*^{R} *cdc2-3w* and *cdc25Δ::ura4*$^{+}$ *cdc2-3w* strains was dissected using a micromanipulator. Colonies formed from germinated spores were replicated on plates with YE plus G418 (selecting for *dnt1Δ::kan*^{R}) and EMM without uracil (selecting for *cdc25Δ::ura4*$^{+}$) (left). Microcolonies corresponding to triple mutant spores are marked by dashed circles and three of them (2A, 3B and 6D) are shown on the right. (D) Live-cell images of calcofluor-stained wild-type, *dnt1Δ*, *cdc25-22* and *dnt1Δ cdc25-22* cells grown in EMM at 25℃. Scale bar: 10 μm. (E) Quantification of cell lengths at cell division. Cells were grown in EMM at 25℃ and $n>200$ cells with septa were measured for each genotype. Data are presented as plots showing the average lengths of septated cells and standard deviation (s.d.) within the cell population for each genotype strain. The numbers in each plot correspond to the mean values of cell length. ***$P<0.001$.

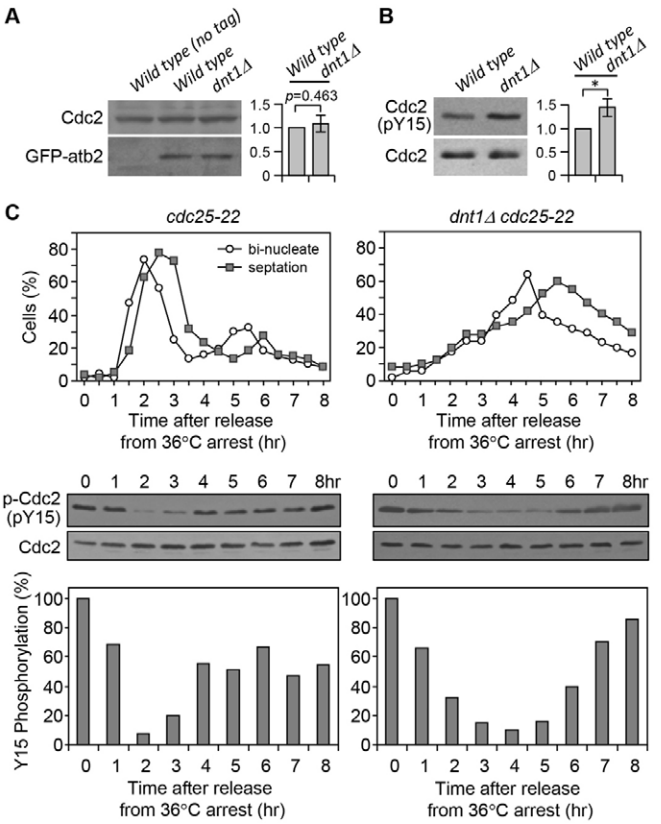

Fig. 2. Dnt1 positively regulates G2/M transition during the cell cycle by affecting the phosphorylation status of Cdc2 kinase. (A) The protein level of Cdc2 is not altered in *dnt1Δ* cells. Protein samples were prepared from wild type without GFP-Atb2, wild type with GFP-Atb2 and *dnt1Δ* GFP-Atb2 strains. Immunoblotting was performed with anti-PSTAIR (top) and anti-GFP (bottom) antibodies to detect total Cdc2 and Atb2, respectively. The levels of Cdc2 were normalized to those of GFP-Atb2 in each strain. $n=3$; $P>0.05$. (B) Phosphorylation of Cdc2 on Tyr^{15} (Y15P) is increased in *dnt1Δ* cells. Immunoblotting was performed with anti-phospho-Cdc2 (Tyr^{15}) (top) and anti-PSTAIR (bottom) antibodies to detect phosphorylated Cdc2 (Y15P) and total Cdc2, respectively. The levels of phosphorylated Cdc2 (Y15P) were normalized to those of total Cdc2 in each strain. $n=3$; *$P<0.05$. (C) G2/M transition and cell cycle progression is delayed in *dnt1Δ* cells. Wild-type (*cdc25-22*) or *dnt1Δ* mutant (*cdc25-22 dnt1Δ*) cells were synchronized at 36℃ for 3.5 hours and then released from the growth arrest by transfer back to 25℃. Aliquots were taken at different time intervals and were either fixed and stained with calcofluor and DAPI, or subjected to immunoblotting with anti-phospho-Cdc2 (Tyr^{15}) and anti-PSTAIR antibodies to detect phosphorylated Cdc2 (Y15P) and total Cdc2, respectively (middle). The percentages of binucleated and septated cells were counted for each time point (top). The levels of phosphorylated Cdc2 (Y15P) were normalized to those of total Cdc2 at each time point, with the relative ratio at time 0 set as 100% (bottom).

Cdc2 Tyr^{15} dephosphorylation during mitosis in *dnt1Δ* cells was extended compared with control cells (Fig. 2C). Taken together, these results suggest that, in fission yeast, Dnt1 positively regulates both G2/M transition and mitotic exit during the cell cycle by affecting the phosphorylation status of Cdc2 kinase.

Dnt1 regulation of the G2/M transition acts through Wee1

Our genetic analyses suggested that the cell cycle defect at G2/M in *dnt1Δ* cells was not dependent on Cdc25. To dissect how Dnt1

facilitates the G2/M progression, we conducted epistasis experiments measuring the cell length at division of double mutants for *dnt1Δ* and a series of genes involved in G2/M transition control (Fig. 3B and supplementary material Fig. S2). Mostly these double mutants either showed additive effect on cell length or divided at an intermediate length. Notably, no increase in cell size at division was observed in *cdc2-1w dnt1Δ, wee1-50 dnt1Δ* and *wee1Δ dnt1Δ* double mutant cells compared with the *cdc2-1w*, *wee1-50* and *wee1Δ* single mutants, respectively (Fig. 3A,B). Cell length measurements also revealed that the longer size at division in the *dnt1Δ* mutant was not dependent on enhanced activity of Clp1 phosphatase or Pom1 kinase, which have been shown to be involved in negatively regulating Cdc25 and Cdr1/2 activity respectively (supplementary material Fig. S2) (Martin and Berthelot-Grosjean, 2009; Moseley and Nurse, 2009; Wolfe and Gould, 2004; Wolfe et al., 2006). These findings suggest that Wee1 is required for Dnt1-mediated cell cycle control during mitotic commitment.

Previous studies have shown that in fission yeast, G2 DNA-damage-checkpoint activation causes G2/M delay and sustained Wee1-mediated Tyr^{15} phosphorylation on Cdc2 until completion of repair (O'Connell et al., 1997; Rhind et al., 1997). Moreover, deletion of the ribosome-associated RACK1 (receptor of activated C kinase) ortholog Cpc2 leads to a Wee1-dependent cell cycle delay at the G2/M transition (Núñez et al., 2010). To investigate the possible functional connection between Dnt1 and the function of either the G2 DNA-damage checkpoint or Cpc2, we examined the cell length of double mutants between *dnt1Δ* and G2 DNA-damage-checkpoint mutants (*rad3Δ*, *chk1Δ*, *cds1Δ* and *tel1Δ*) and *cpc2Δ*. As shown in supplementary material Fig. S3A, all double mutants divided at an intermediate cell length, suggesting that Dnt1 does not regulate these pathways. Consistent with these observations, we found that G2 DNA-damage-checkpoint mutants did not counteract the suppressive effect of *dnt1Δ* on SIN mutant *cdc14-118*. Moreover, *cpc2Δ* further elongated the length of *dnt1Δ* cells and enhanced the rescue of the *cdc14-118* mutant by *dnt1Δ*, showing an additive effect (supplementary material Fig. S3B,C, and data not shown).

Recently, we have shown that during metaphase Dnt1 interacts with and inhibits Dma1 (Wang et al., 2012). Previous studies have shown that Dma1 localizes to the SPB through interaction with the SIN scaffold protein Sid4 and it ubiquitylates Sid4 to prevent recruitment of the Polo-like kinase and the SIN activator Plo1 to SPBs during a mitotic checkpoint arrest (Guertin et al., 2002b; Johnson and Gould, 2011). It is also known that the SPB component Cut12 is functionally linked with

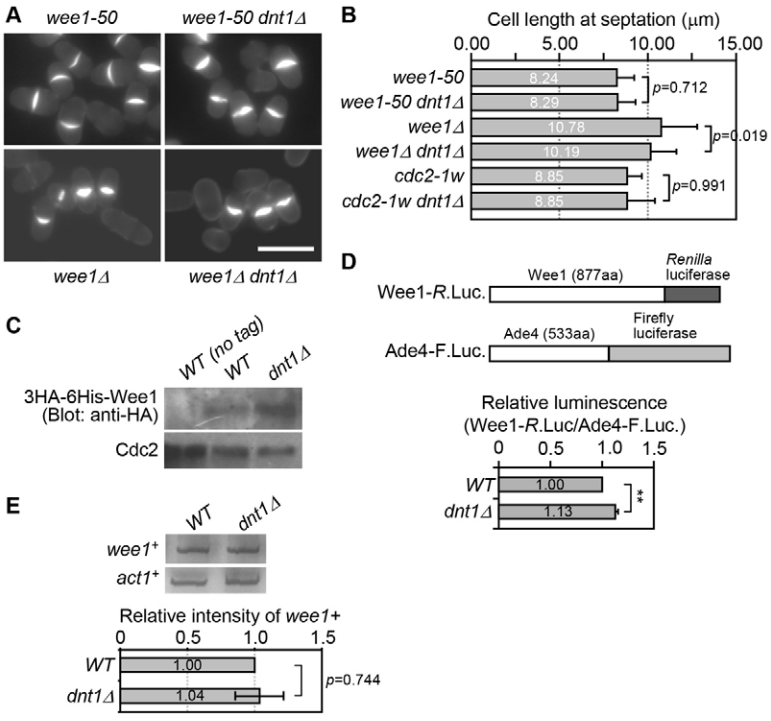

Fig. 3. Dnt1 controls G2/M transition by negatively regulating Wee1 protein levels. (A) Live-cell images of calcofluor-stained *wee1-50*, *wee1-50 dnt1Δ*, *wee1Δ* and *wee1Δ dnt1Δ* cells. Cells were first grown in YE at 25℃ and then shifted to 37℃ for 4 hours (for *wee1-50* and *wee1-50 dnt1Δ*) or grown in EMM at 25℃ (for *wee1Δ* and *wee1Δ dnt1Δ*) before calcofluor staining and photography. Scale bar: 10 μm. (B) Quantification of cell lengths at cell division. Cells were grown in either YE at 25℃ and then shifted to 37℃ for 4 hours (for *wee1-50* and *wee1-50 dnt1Δ*) or grown in EMM at 25℃ (for *wee1Δ*, *wee1Δ dnt1Δ*, *cdc2-1w* and *cdc2-1w dnt1Δ*). $n>200$ cells with septa were measured for each strain. (C,D) Wee1 protein levels are elevated in *dnt1Δ* cells. (C) Wild-type strains without or with *3HA-6His-Wee1* and *dnt1Δ 3HA-6His-Wee1* strain were grown in YE medium to mid log phase and then subject to protein extraction and immunoblotting with anti-HA antibody to detect Wee1. Cdc2 was used as loading control. (D) Wee1 luciferase activity was analyzed using Wee1-R.luciferase and Ade4-F.luciferase assay system in wild-type and *dnt1Δ* cells. The schematic depiction of Wee1-R.luciferase and Ade4-F.luciferase constructs is shown (top). Cells were collected from cultures grown in YE at 30℃. Wee1-R.luciferase and Ade4-F.luciferase activity was measured and the relative luminescence was quantified with ratio between Wee1-R.luciferase and Ade4-F.luciferase activity in wild-type cells being set as 1.00 (bottom). $n=3$; $^{**}P<0.01$. (E) $wee1^+$ mRNA level is unchanged in *dnt1Δ* cells. Total RNA was extracted from wild-type and *dnt1Δ* cells and subject to RT-PCR. PCR products were resolved in PAGE gels and then silver stained (top). The levels of $wee1^+$ mRNA were normalized to those of $act1^+$ (internal control) and the relative ratio in wild-type cells was set as 1.00 (bottom). $n=3$; $P>0.05$.

Plo1. The gain-of-function mutant *cut12-S11* promotes Plo1 recruitment to the G2 phase SPB, boosts global Plo1 activity and drives advanced mitotic commitment (Bridge et al., 1998; Grallert et al., 2013). To examine whether Cut12 or Dma1-regulated Plo1 is involved in Dnt1 modulation of G2/M transition, we first measured the cell length of double mutants between *dnt1Δ* and *cut12-S11* or *dma1Δ*, and found that neither of these mutants could reverse the longer size at division of *dnt1Δ* cells (supplementary material Fig. S4A). Moreover, neither *cut12-S11* nor *dma1Δ* could rescue the synthetic lethality of *dnt1Δ cdc25-22* double mutant (supplementary material Fig. S4B). Therefore, the G2/M transition defects in *dnt1Δ* cells are not linked to Cut12- or Dma1-controlled Plo1.

Wee1 protein is upregulated in *dnt1Δ* cells

Our epistasis analyses suggested that the G2/M delay in *dnt1Δ* cells most likely acts through Wee1 to promote maintenance of Cdc2 Tyr^{15} phosphorylation. This Cdc2 inhibitory effect could be exerted by increasing Wee1 activity and/or Wee1 abundance. To gain insight into the mechanism by which Wee1 inhibits Cdc2 when *dnt1*$^+$ is absent, we determined Wee1 protein levels in the wild-type and *dnt1Δ* strains expressing a genomic version of HA_3His_6-Wee1 (Raleigh and O'Connell, 2000). Although we occasionally observed an increase of HA_3His_6-Wee1 levels in *dnt1Δ* cells compared with wild-type cells (Fig. 3C), we experienced some technical difficulty with the reproducibility of these assays. Therefore, we turned to a newly developed strategy to monitor protein levels by tagging Wee1 with luciferase from the sea pansy *Renilla reniformis* (or R.luciferase) (Matthews et al., 1977), while using firefly-luciferase-tagged Ade4 (Ade4-F.luciferase) as an internal control (see Fig. 3D, top panel). By using this strategy we found a reproducibly significant increase of Wee1 protein levels in *dnt1Δ* cells compared with wild-type cells (Fig. 3D, bottom panel). Therefore, Dnt1 negatively affects the abundance of Wee1 kinase, which is a negative regulator of Cdk1.

To understand how Wee1 protein is affected by Dnt1, we examined the mRNA levels of the *wee1*$^+$ gene in *dnt1Δ* cells by RT-PCR. As shown in Fig. 3E, our results showed that the increase in Wee1 protein levels observed in *dnt1Δ* cells did not result from enhanced expression of *wee1*$^+$ mRNA. Thus, it is possible that Dnt1 might influence the stability and/or turnover of Wee1 protein. The observation that Wee1 is upregulated in *dnt1Δ* cells led us to explore the possibility that protein levels of various Cdk1 regulators, such as Cdc25, Cdc13 (cyclin B), Pom1, Cdr1 or Cdr2 might be altered in this mutant. However, none of these proteins was affected by deletion of *dnt1*$^+$ (supplementary material Fig. S5 and data not shown).

Elevated Wee1 levels are responsible for the rescue of compromised SIN mutants by *dnt1Δ*

We addressed the functional significance of the negative regulation of Wee1 by Dnt1 during activation of SIN signaling by exploring how *wee1*$^+$ affects the rescue of SIN mutants by *dnt1Δ*. Maximal SIN activation depends upon Cdk1 inhibition and thus SIN mutants are very sensitive to high Cdk1 activity. Thus, it is plausible that the low Cdk1 activity promoted by elevated Wee1 levels in *dnt1Δ* cells might be sufficient to maintain the SIN signaling activity to certain degree. To test this possibility, we first examined whether elevated Wee1 levels alone could rescue SIN mutants. Intriguingly, we found that a slight elevation of Wee1 levels by using a P_{81nmt1}-GFP-Wee1 construct rescued the SIN mutant *cdc14-118* to a similar extent as *dnt1Δ* (Fig. 4A). Next, we introduced the *wee1Δ* mutation into single SIN mutants (*cdc14-118* and *sid2-250*) or double mutants with *dnt1Δ* (*dnt1Δ cdc14-118* and *dnt1Δ sid2-250*), and monitored either growth at different temperatures or the accumulation of multinucleated cells after a shift to 37℃ in liquid cultures (Fig. 4B,C). Strikingly, *wee1Δ* completely abolished rescue of SIN mutants by *dnt1Δ*, as indicated by the similar temperature sensitivity and rate of multinucleated cells between SIN and *wee1Δ dnt1Δ* SIN strains (Fig. 4B,C). We also observed that the *wee1Δ* completely abolished rescue of the

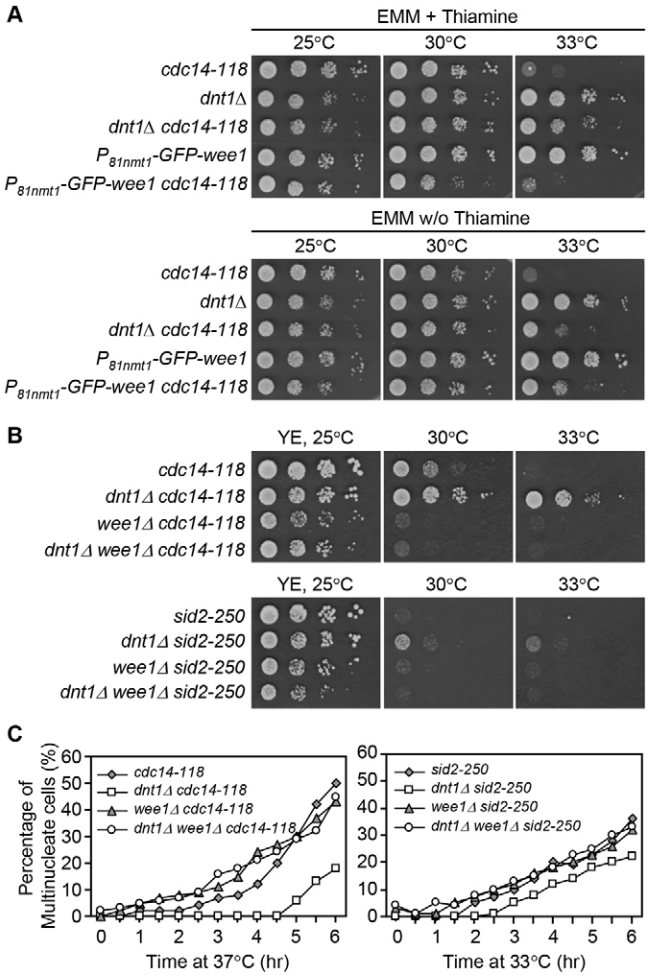

Fig. 4. Rescue of compromised SIN mutants by *dnt1Δ* is abolished by deletion of *wee1*$^+$. (A) Slightly elevated Wee1 levels rescue a *cdc14-118* mutant. Serial dilutions (10-fold) of the indicated strains were spotted on EMM with or without thiamine after being grown in YE and then washed by EMM liquid and incubated at the indicated temperatures. (B,C) Rescue of SIN mutants by *dnt1Δ* is dependent on the presence of *wee1*$^+$. (B) Serial dilutions (10-fold) of the indicated strains were spotted on YE plates and incubated for 3–5 days at the indicated temperatures before being photographed. (C) Single, double and triple mutant cells with indicated genotypes were first grown in YE at 25℃, and then they were shifted to 37℃ (for *cdc14-118* mutants; left) or 33℃ (for *sid2-250* mutants; right). Cells were sampled every 30 minutes for a period of 6 hours, fixed and stained with DAPI. $n>200$ cells were counted at each time point and the frequencies of cells with multiple nuclei (as indication of cytokinetic defects) were quantified.

actomyosin ring formation mutant *cdc8-110* by *dnt1Δ* (supplementary material Fig. S6). Furthermore, rescue of SIN mutants by *dnt1Δ* was not affected by either *dma1Δ* or *cut12-S11* (supplementary material Fig. S7), suggesting that Dma1- or Cut12-controlled Plo1 is not involved in SIN regulation by Dnt1. These results allow us to conclude that rescue of compromised SIN mutants by *dnt1Δ* is solely dependent on elevated Wee1 levels and the concomitant attenuation of Cdk1 activity.

Dnt1 functions in parallel with SCF to regulate Wee1 degradation

The finding that the absence of *dnt1*$^+$ leads to increased Wee1 levels prompted us to investigate the possible mechanism involved in this alteration. We anticipated that Dnt1 might influence the turn-over rate of Wee1. It has been shown that the SCF complex is responsible for Wee1 degradation at the onset of M phase in budding yeast, frog and human cells (Kaiser et al., 1998; Michael and Newport, 1998; Watanabe et al., 2004). Therefore, we first examined whether SCF is also required for Wee1 degradation in fission yeast. Wee1 protein stability was measured with Wee1-R.luciferase activity in the 26S proteasome subunit mutant *mts3-1* (Seeger et al., 1996), and temperature-sensitive mutant *skp1-A7*, which carries a mutation (T454C) in the major SCF subunit Skp1 (Lehmann et al., 2004). We found that Wee1 protein was more abundant in *mts3-1* and *skp1-A7* cells than in wild-type cells at the restrictive temperature (Fig. 5A), suggesting that the SCF-mediated proteasome-dependent pathway is responsible for Wee1 proteolysis in fission yeast.

To further explore whether Dnt1 influences SCF-mediated Wee1 degradation, we measured Wee1-R.luciferase activity and cell length at division in *skp1-A7 dnt1Δ* double mutant cells. We observed that *dnt1Δ* further enhanced Wee1 protein stability and cell elongation in the *skp1-A7* mutant (Fig. 5A,B). These data suggest that Dnt1 probably does not directly affect SCF-mediated Wee1 degradation.

We also noticed that the elevated Wee1 protein level caused by *skp1-A7* mutation could rescue SIN mutants to a similar degree as *dnt1Δ*, and the triple mutant *skp1-A7 dnt1Δ cdc14-118* showed an even lower rate of accumulation of multinucleate cells (Fig. 5C,D). It is noteworthy that the *skp1-A7* mutation did not rescue *cdc14-118* more effectively than *dnt1Δ*, although the *skp1-A7* mutant had increased levels of Wee1. This is probably due to the thermosensitivity of the *skp1-A7* mutation, which could make *cdc14-118* cells sicker. Nonetheless, these data are consistent with the idea that Dnt1 works in parallel with SCF to regulate the rate of Wee1 protein turn-over.

Discussion

Previously, we identified the nucleolar protein Dnt1 as an inhibitor of the SIN signaling in fission yeast (Jin et al., 2007), but its exact role and mechanism of action in the regulation of SIN remained unclear. Here, we show that deletion of *dnt1*$^+$ leads to an increased abundance of the Cdk1 inhibitor Wee1 kinase and thus suppresses Cdk1 activity and causes a G2/M transition delay. The ability of *dnt1Δ* to lower Cdk1 activity through Wee1 is responsible for the rescue of SIN mutants, because deletion of the *wee1*$^+$ gene completely abolished elevated SIN signaling caused by *dnt1Δ*. Hence, we have uncovered a novel mechanism by which Dnt1 controls SIN signaling during late mitosis through its effect on Cdk1 activity.

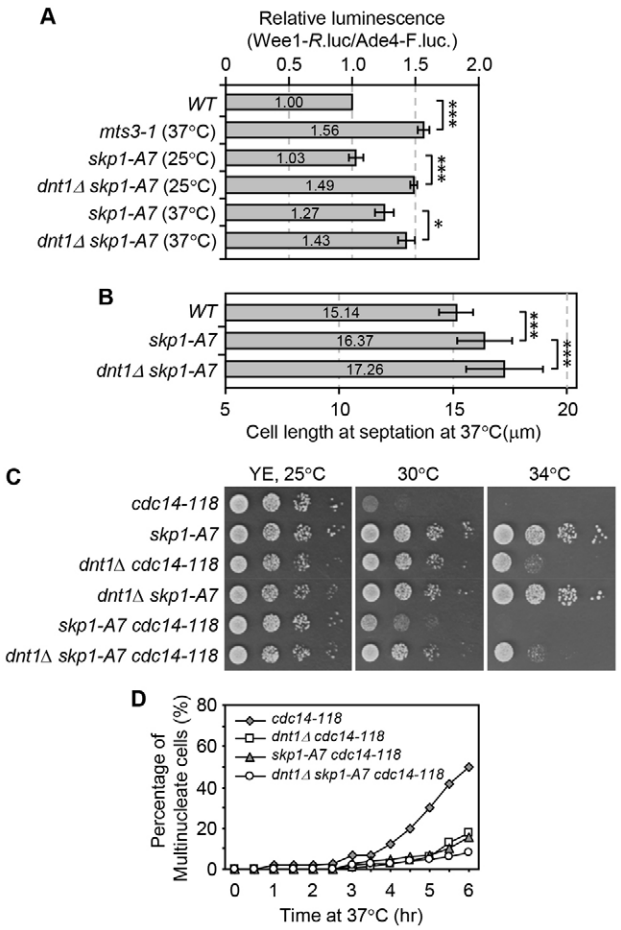

Fig. 5. Dnt1 functions in parallel with SCF to regulate Wee1 degradation. (A) Wee1 luciferase activity was analyzed using Wee1-R.luciferase and Ade4-F.luciferase assay system in wild-type and mutant cells with indicated genotypes, as described in Fig. 3D. Cells were collected from cultures grown in YE at either 25℃ or 37℃ for 4 hours. ***$P<0.001$, *$P<0.05$. (B) Quantification of cell lengths at cell division. Cells were first grown in YE at 25℃ and then shifted to 37℃ for 4 hours before being imaged. $n>200$ cells with septa were measured for each strain. ***$P<0.001$. (C) Serial dilutions (10-fold) of the indicated strains were performed as in Fig. 4B. (D) The frequencies of cells containing multiple nuclei (as an indication of cytokinetic defects) were quantified in single, double and triple mutants with indicated genotypes, as described in Fig. 4C.

Negative correlation between SIN signaling and Cdk1 activity

Initiation of cytokinesis is the final crucial event of the cell cycle, and it must be tightly coordinated with completion of chromosome segregation. In fission yeast, the timing of cytokinesis is regulated by the SIN signaling pathway. Studies performed with this organism have lent support to the notion that SIN signaling is negatively regulated by Cdk1 activity, and that maximum SIN activation depends upon Cdk1 inactivation. For example, an early study showed that inactivation of Cdk1 by *cdc2-33* mutation promotes cytokinesis and septum formation even in metaphase-arrested cells induced by overexpression of the spindle assembly checkpoint protein Mad2 (He et al., 1997). Subsequently, another study confirmed that loss of Cdc2 activity in these metaphase-arrested cells was sufficient to allow SIN

kinase complex Sid1–Cdc14 to localize at one SPB and to promote cytokinesis onset (Guertin et al., 2000). More recently, it has been shown that inactivation of Cdk1 using an analogue-sensitive mutant allele *cdc2-as* promotes the asymmetrical distribution of SIN proteins (Sid1 and Cdc7) to the spindle poles, and the recruitment of the most downstream SIN component Mob1 and β-(1,3) glucan synthase to the contractile ring (Dischinger et al., 2008). Conversely, high Cdk1 activity caused by increased expression of nondegradable Cdc13 (cyclin B) blocked cells in anaphase and prevented SIN kinase Cdc7 from becoming asymmetrically localized to one SPB during anaphase B; it also blocked all subsequent relocalization events in the SIN and therefore inhibited septation (Chang et al., 2001; Yamano et al., 1996).

The negative-feedback control of cytokinesis by Cdk1 activity is not restricted to fission yeast and is conserved in all eukaryotes from yeasts to vertebrates. In another model organism, budding yeast *S. cerevisiae*, inactivation of Cdk1 in cells arrested by expression of a non-degradable *CLB2* promotes mitotic exit and cytokinesis (Ghiara et al., 1991). Inactivation of Cdk1 is also required for localization of the vesicle fusion machinery to the bud neck during mitotic exit and cytokinesis (VerPlank and Li, 2005). Recently, it has been shown that Cdk1 is asymmetrically localized to mother SPBs during early anaphase and inhibits Cdc15 (orthologous to *S. pombe* Cdc7) and thus MEN signaling activation (König et al., 2010). In dividing cultured human cells, inhibition of Cdk1 by selective small-molecule inhibitors also caused premature cytokinesis, indicating that Cdk1 activity is necessary and sufficient for maintaining the mitotic state of the cells and preventing premature cytokinesis (Vassilev et al., 2006). However, the detailed mechanism involved in this control is not entirely understood.

Thus, the data obtained from all model organisms studied to date point to a universal requirement for inactivation of CDK1 to promote cytokinesis. This control mechanism is regarded as the ideal coupling between nuclear and cell division. However, so far, only two budding yeast proteins involved in mitotic exit and cytokinesis, CDC15 and MOB1, have been confirmed to be phosphorylated by Cdk1 (Jaspersen and Morgan, 2000; König et al., 2010). Whether homologues of these proteins in other organisms (such as Cdc7 and Mob1 in fission yeast, or Mst2 and Mob1 in *Drosophila* and vertebrates (reviewed by Doxsey et al., 2005) are also phosphorylated by Cdk1 remains to be demonstrated. Further studies will be required to identify and define the complete repertoire of Cdk1 substrates influencing the timing of cytokinesis in fission yeast and higher eukaryotes.

Nucleolar-protein-mediated control of Cdk1 activity and cytokinesis

Dnt1 is not the first nucleolar protein identified in fission yeast to be involved in regulating both Cdk1 activity and SIN signaling. Another nucleolar protein, the Cdc14 phosphatase family member Clp1, is a well-studied example of such regulation. At the end of mitosis, Clp1 reverses Cdk1-dependent phosphorylation of Cdc25 and destabilizes and inactivates Cdc25 by promoting recognition of Cdc25 by two ubiquitin E3 ligases, the anaphase-promoting complex/cyclosome (APC/C) (RING-type) and Pub1/Pub2 (HECT-type) (Esteban et al., 2004; Esteban et al., 2008; Wolfe and Gould, 2004). Thus, stabilized Cdc25 allows *clp1Δ* cells to delay mitotic Cdk1 inactivation at the end of mitosis and advance into G2 (Wolfe and Gould, 2004). Moreover, SIN signaling is probably antagonized by persistent Cdk1 activity. In addition to its role in affecting timely Cdk1 inactivation, Clp1 also directly contributes to robust and successful cytokinesis, particularly when the cell division machinery (such as the actomyosin ring) is slightly perturbed or damaged (Mishra et al., 2004). A recent study revealed that Clp1 is tethered at the contractile ring (CR) through its association with the anillin-related protein Mid1, and regulates CR protein dynamics and mobility by dephosphorylating CR components Cdc15 and possibly Myo2 (myosin II heavy chain) (Clifford et al., 2008).

Cdc14-family phosphatases are conserved in all eukaryotes examined so far, but have been best studied in both budding and fission yeasts. The negative regulation of Cdk1 at late mitosis represents a conserved feature of Cdc14 phosphatase family members (for reviews see D'Amours and Amon, 2004; Krapp et al., 2004; Mocciaro and Schiebel, 2010; Stegmeier and Amon, 2004). Budding yeast ScCdc14 and fission yeast Clp1 are regulated in part by their cell-cycle-dependent changes in localization, with both proteins thought to be sequestered and inactivated in the nucleolus during interphase. The activity of ScCdc14 is controlled by its association with the competitive inhibitor Cfi1/Net1, and only during anaphase is ScCdc14 released from its inhibitor to spread into the nucleus and cytoplasm, allowing the dephosphorylation of its substrates (reviewed by Mocciaro and Schiebel, 2010; Stegmeier and Amon, 2004). In contrast to ScCdc14, both Clp1 and mammalian Cdc14B are released from the nucleolus upon entry into mitosis (Cho et al., 2005; Cueille et al., 2001; Nalepa and Harper, 2004; Trautmann et al., 2001), but how this process is regulated is currently unknown. Although the amino acid sequence of Dnt1 shows weak similarity to that of budding yeast Net1/Cfi1 and it has been speculated that Dnt1 might function as a nucleolar inhibitor of Clp1 (Jin et al., 2007), the present study demonstrates that Dnt1 actually influences Wee1 stability and thus Cdk1 activity. Therefore, there are at least two parallel pathways emerging from the nucleolus which converge at Cdk1 to regulate SIN signaling: one including both Dnt1 and Wee1, and another involving Clp1-controlled Cdc25 (Fig. 6).

Our findings also suggest that SCF-mediated degradation of Wee1 is probably conserved in fission yeast, although the direct evidence of Wee1 ubiquitylation by SCF is currently lacking. The elucidation of the specific mechanism by which Dnt1 controls

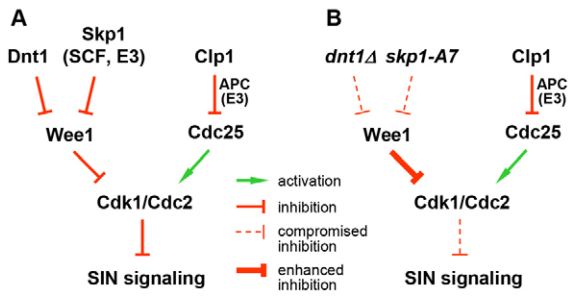

Fig. 6. Model depicting how Dnt1- and Clp1-dependent modulation of Wee1 and Cdc25, respectively, converge at Cdk1 to regulate SIN signaling. Signaling flows in wild-type cells (A) and *dnt1Δ* or *skp1-A7* mutants (B) are summarized.

degradation of Wee1 remains a mystery and merits further investigation.

Materials and Methods

General yeast strains, media and growth conditions

Fission yeast strains used in this study were constructed by standard techniques (Moreno et al., 1991) and are listed in supplementary material Table S1. *S. pombe* strains were grown in rich medium [yeast extract (YE)] or Edinburgh minimal medium (EMM) with appropriate supplements (Moreno et al., 1991). EMM with 5 μg/ml thiamine was used to repress expression from the *nmt1* promoter. YE containing 100 mg G418 (Sigma) or nourseothiricin (clonNAT) (Werner BioAgents) per liter was used for selecting kan^R and nat^R cells, respectively. For serial-dilution drop tests for growth, three serial 10-fold dilutions were made and 5 μl of each was spotted on plates with the starting cell number of 10^4. Cells were pre-grown in liquid YE or EMM at 25℃ until they reached exponential phase and were then spotted onto YE or EMM plates at the indicated temperatures and incubated for 3 to 5 days before scanning. In block-and-release experiments performed with *cdc25-22* mutant strains, the cells were grown in YES medium to an A_{600} of 0.2 at 25℃ (permissive temperature), shifted to 36℃ for 3.5 hours, and then released from the growth arrest by transfer back to 25℃.

Construction of epitope-tagged strains carrying Ade4-F.luciferase and Wee1-R.luciferase and luciferase-activity assay

Firefly and *Renilla* Luciferase lacking start codons were cloned from the pGL3 and pRL-TK plasmids (Promega) into pFA6a plasmid carrying either kan^R or nat^R selection marker. These plasmids were used to add C-terminal epitope tags to the endogenous locus to create Ade4-F.luciferase (kan^R) and Wee1-R.luciferase (nat^R) alleles using PCR-based gene targeting (Bähler et al., 1998). Candidate transformants by homologous recombination were selected by growth on selective plates containing G418 or ClonNAT and subsequently confirmed by PCR analysis.

Western blot analyses

Yeast cell extracts were prepared in lysis buffer (120 mM Tris-HCl, pH 6.8, 4% SDS, 20% glycerol, 8M urea, 0.6 M β-mercaptoethanol) by glass bead disruption using FastPrep homogenizer (MP Biomedical), and denatured in 2× SDS sample buffer (100 mM Tris-HCl, pH 6.8, 4% SDS, 20% glycerol, 0.2% Bromophenol Blue, 0.6 M β-mercaptoethanol) before being resolved on 8–12% SDS-PAGE gels. For detection, mouse monoclonal anti-GFP (Roche), rabbit polyclonal anti-Myc (GeneScript), rat monoclonal anti-HA (Roche) and rabbit polyclonal anti-Cdc2 (Tyr^{15}) (sc-7989-R, Santa Cruz Biotechnology) were used as the primary antibodies (1:1000–1:2000 dilutions). Cdc2 or GFP-atb2 was detected using rabbit polyclonal anti-PSTAIRE (sc-53, Santa Cruz Biotechnology) or mouse monoclonal anti-GFP (Roche), respectively, as loading controls (1:1000 dilution). Goat anti-mouse, anti-rabbit or anti-rat conjugated to horseradish peroxidase (Pierce) was used as the secondary antibody at 1:10,000 dilution. Membranes were developed with ECL western blotting reagents (Pierce). Protein levels were quantified using ImageJ software (National Institutes of Health, Bethesda, MD) with Cdc2 or GFP-atb2 as a loading control.

Luciferase activity assay in yeast cell lysate

Yeast strains carrying both Ade4-F.luciferase (kan^R) and Wee1-R.luciferase (nat^R) were used. Exponential phase cultures were pre-grown in liquid YE at 30℃, 25℃ or shifted from 25℃ to 37℃ for 4 hours, and 1–10×10^7 cells were collected and washed once with sterile water. Cell lysates were prepared in 100–200 μl cold 1× passive Lysis Buffer (PLB) by glass bead disruption using FastPrep homogenizer. Firefly and *Renilla* luciferase activities in cell lysates were measured using the Dual-Reporter Assay System (Promega) following instructions provided by the manufacturer.

RT-PCR and silver staining

Total RNA was isolated from yeast cells grown in YES liquid medium to an A_{600} of <0.4 and disrupted with FastPrep homogenizer by using the TRI Reagent Solution (TRIZOL) (TaKaRa Bio) and following the manufacturer's instructions. RT was performed with Prime-Script RT reagent Kit (TaKaRa) at 37℃ for 15 minutes followed by treatment at 85℃ for 5 seconds. Primer pairs to detect $wee1^+$ and $act1^+$ transcripts by PCR were as follows: wee1-2189 bp-F, 5′- GT-GAATACATTGCGCGTAAG-3′ and wee1-2540 bp-R, 5′-CTACGCATTTCAA-CCCAGC-3′ (amplifying a 400 bp fragment); act1-F, 5′-GTATGCCTCTGGTC-GTACCAC-3′ and act1-R, 5′-CAATTTCACGTTCGGCGGTAG-3′ (amplifying a 200 bp fragment). PCR products were then resolved by 5% Tris-acetate-EDTA PAGE (TAE-PAGE). The gels were stained with 0.25% $AgNO_3$ and scanned and images were processed with Adobe Photoshop software and the intensities of PCR products were quantified using ImageJ software with $act1^+$ transcript as an internal control.

Microscopy

GFP-fusion proteins were observed in cells after fixation with cold methanol or in live cells. For DAPI (4′, 6-diamidino-2-phenylindole, Sigma) staining of nuclei, cells were fixed with cold methanol, washed in PBS and resuspended in PBS plus 1 μg/ml DAPI. To determine cell size at division the yeast strains were grown in either EMM2 or YES medium to an A_{600} of <0.5 and treated with Calcofluor white (CW, Sigma) at 50 μg/ml final concentration, which specifically stains cell wall and septum. A minimum of 100 septated cells were scored for each mutant. Photomicrographs were obtained using a Nikon 80i fluorescence microscope coupled to a cooled CCD camera (Hamamatsu, ORCA-ER) and image processing, analysis and cell length measurement were carried out using Element software (Nikon) and Adobe Photoshop.

Statistical analysis

All experiments were repeated at least three times with similar results. In order to determine statistical significance of our data, two tailed Student's *t*-tests were performed, and $P<0.05$ was considered statistically significant.

Acknowledgements

We are grateful to Drs Kathleen L. Gould, Mohan K. Balasubramanian, Dannel McCollum, Jianhua Liu, Paul Russell, Iain Hagan, Takashi Toda, Janni Petersen, James Moseley and the Yeast Genetic Resource Center Japan (YGRC) for providing yeast strains or plasmids.

Author contributions

Y.W. and Q.W.J. conceived the project and designed the experiments; Z.Y.Y., M.T.Z., G.Y.W., D.X., D.K., A.F., J.C. and H.M. performed the experiments; Z.Y.Y., J.C., H.M., N.R., Y.W. and Q.W.J. analyzed data; Y.W. and Q.W.J. wrote the paper.

Funding

This work was supported by the National Institutes of Health [grant number GM-069957 to N.R.]; MEC European Regional Development Fund co-funding from the EU [grant number BFU2011-22517 to J.C.]; the National Natural Science Foundation of China [grant number 31171298 to Q.W.J.]; Key Project of the Chinese Ministry of Education [grant number 108076 to Q.W.J.]; the 111 Project of Education of China [number B06016]. Deposited in PMC for release after 12 months.

Supplementary material available online at
http://jcs.biologists.org/lookup/suppl/doi:10.1242/jcs.132845/-/DC1

References

Aligue, R., Wu, L. and Russell, P. (1997). Regulation of Schizosaccharomyces pombe Wee1 tyrosine kinase. *J. Biol. Chem.* **272**, 13320-13325.

Bähler, J., Wu, J. Q., Longtine, M. S., Shah, N. G., McKenzie, A., 3rd, Steever, A. B., Wach, A., Philippsen, P. and Pringle, J. R. (1998). Heterologous modules for efficient and versatile PCR-based gene targeting in Schizosaccharomyces pombe. *Yeast* **14**, 943-951.

Balasubramanian, M. K., Bi, E. and Glotzer, M. (2004). Comparative analysis of cytokinesis in budding yeast, fission yeast and animal cells. *Curr. Biol.* **14**, R806-R818.

Berry, L. D. and Gould, K. L. (1996). Regulation of Cdc2 activity by phosphorylation at T14/Y15. *Prog. Cell Cycle Res.* **2**, 99-105.

Bridge, A. J., Morphew, M., Bartlett, R. and Hagan, I. M. (1998). The fission yeast SPB component Cut12 links bipolar spindle formation to mitotic control. *Genes Dev.* **12**, 927-942.

Callegari, A. J. and Kelly, T. J. (2007). Shedding light on the DNA damage checkpoint. *Cell Cycle* **6**, 660-666.

Calonge, T. M., Eshaghi, M., Liu, J., Ronai, Z. and O'Connell, M. J. (2010). Transformation/transcription domain-associated protein (TRRAP)-mediated regulation of Wee1. *Genetics* **185**, 81-93.

Chang, L., Morrell, J. L., Feoktistova, A. and Gould, K. L. (2001). Study of cyclin proteolysis in anaphase-promoting complex (APC) mutant cells reveals the requirement for APC function in the final steps of the fission yeast septation initiation network. *Mol. Cell. Biol.* **21**, 6681-6694.

Cho, H. P., Liu, Y., Gomez, M., Dunlap, J., Tyers, M. and Wang, Y. (2005). The dual-specificity phosphatase CDC14B bundles and stabilizes microtubules. *Mol. Cell. Biol.* **25**, 4541-4551.

Clifford, D. M., Wolfe, B. A., Roberts-Galbraith, R. H., McDonald, W. H., Yates, J. R., 3rd and Gould, K. L. (2008). The Clp1/Cdc14 phosphatase contributes to the

robustness of cytokinesis by association with anillin-related Mid1. *J. Cell Biol.* **181**, 79-88.

Craven, R. A., Griffiths, D. J., Sheldrick, K. S., Randall, R. E., Hagan, I. M. and Carr, A. M. (1998). Vectors for the expression of tagged proteins in Schizosaccharomyces pombe. *Gene* **221**, 59-68.

Cueille, N., Salimova, E., Esteban, V., Blanco, M., Moreno, S., Bueno, A. and Simanis, V. (2001). Flp1, a fission yeast orthologue of the s. cerevisiae CDC14 gene, is not required for cyclin degradation or rum1p stabilisation at the end of mitosis. *J. Cell Sci.* **114**, 2649-2664.

D'Amours, D. and Amon, A. (2004). At the interface between signaling and executing anaphase—Cdc14 and the FEAR network. *Genes Dev.* **18**, 2581-2595.

Daga, R. R. and Jimenez, J. (1999). Translational control of the cdc25 cell cycle phosphatase: a molecular mechanism coupling mitosis to cell growth. *J. Cell Sci.* **112**, 3137-3146.

Dischinger, S., Krapp, A., Xie, L., Paulson, J. R. and Simanis, V. (2008). Chemical genetic analysis of the regulatory role of Cdc2p in the S. pombe septation initiation network. *J. Cell Sci.* **121**, 843-853.

Doxsey, S., McCollum, D. and Theurkauf, W. (2005). Centrosomes in cellular regulation. *Annu. Rev. Cell Dev. Biol.* **21**, 411-434.

Esteban, V., Blanco, M., Cueille, N., Simanis, V., Moreno, S. and Bueno, A. (2004). A role for the Cdc14-family phosphatase Flp1p at the end of the cell cycle in controlling the rapid degradation of the mitotic inducer Cdc25p in fission yeast. *J. Cell Sci.* **117**, 2461-2468.

Esteban, V., Sacristán, M., Andrés, S. and Bueno, A. (2008). The Flp1/Clp1 phosphatase cooperates with HECT-type Pub1/2 protein-ubiquitin ligases in Schizosaccharomyces pombe. *Cell Cycle* **7**, 1269-1276.

Fantes, P. A. (1981). Isolation of cell size mutants of a fission yeast by a new selective method: characterization of mutants and implications for division control mechanisms. *J. Bacteriol.* **146**, 746-754.

Ghiara, J. B., Richardson, H. E., Sugimoto, K., Henze, M., Lew, D. J., Wittenberg, C. and Reed, S. I. (1991). A cyclin B homolog in S. cerevisiae: chronic activation of the Cdc28 protein kinase by cyclin prevents exit from mitosis. *Cell* **65**, 163-174.

Gould, K. L. and Simanis, V. (1997). The control of septum formation in fission yeast. *Genes Dev.* **11**, 2939-2951.

Grallert, A., Patel, A., Tallada, V. A., Chan, K. Y., Bagley, S., Krapp, A., Simanis, V. and Hagan, I. M. (2013). Centrosomal MPF triggers the mitotic and morphogenetic switches of fission yeast. *Nat. Cell Biol.* **15**, 88-95.

Guertin, D. A., Chang, L., Irshad, F., Gould, K. L. and McCollum, D. (2000). The role of the sid1p kinase and cdc14p in regulating the onset of cytokinesis in fission yeast. *EMBO J.* **19**, 1803-1815.

Guertin, D. A., Trautmann, S. and McCollum, D. (2002a). Cytokinesis in eukaryotes. *Microbiol. Mol. Biol. Rev.* **66**, 155-178.

Guertin, D. A., Venkatram, S., Gould, K. L. and McCollum, D. (2002b). Dma1 prevents mitotic exit and cytokinesis by inhibiting the septation initiation network (SIN). *Dev. Cell* **3**, 779-790.

Hachet, O., Berthelot-Grosjean, M., Kokkoris, K., Vincenzetti, V., Moosbrugger, J. and Martin, S. G. (2011). A phosphorylation cycle shapes gradients of the DYRK family kinase Pom1 at the plasma membrane. *Cell* **145**, 1116-1128.

He, X., Patterson, T. E. and Sazer, S. (1997). The Schizosaccharomyces pombe spindle checkpoint protein mad2p blocks anaphase and genetically interacts with the anaphase-promoting complex. *Proc. Natl. Acad. Sci. USA* **94**, 7965-7970.

Jaspersen, S. L. and Morgan, D. O. (2000). Cdc14 activates cdc15 to promote mitotic exit in budding yeast. *Curr. Biol.* **10**, 615-618.

Jin, Q. W., Ray, S., Choi, S. H. and McCollum, D. (2007). The nucleolar Net1/Cfi1-related protein Dnt1 antagonizes the septation initiation network in fission yeast. *Mol. Biol. Cell* **18**, 2924-2934.

Johnson, A. E. and Gould, K. L. (2011). Dma1 ubiquitinates the SIN scaffold, Sid4, to impede the mitotic localization of Plo1 kinase. *EMBO J.* **30**, 341-354.

Kaiser, P., Sia, R. A., Bardes, E. G., Lew, D. J. and Reed, S. I. (1998). Cdc34 and the F-box protein Met30 are required for degradation of the Cdk-inhibitory kinase Swe1. *Genes Dev.* **12**, 2587-2597.

Keeney, J. B. and Boeke, J. D. (1994). Efficient targeted integration at leu1-32 and ura4-294 in Schizosaccharomyces pombe. *Genetics* **136**, 849-856.

Kellogg, D. R. (2003). Wee1-dependent mechanisms required for coordination of cell growth and cell division. *J. Cell Sci.* **116**, 4883-4890.

König, C., Maekawa, H. and Schiebel, E. (2010). Mutual regulation of cyclin-dependent kinase and the mitotic exit network. *J. Cell Biol.* **188**, 351-368.

Krapp, A. and Simanis, V. (2008). An overview of the fission yeast septation initiation network (SIN). *Biochem. Soc. Trans.* **36**, 411-415.

Krapp, A., Gulli, M. P. and Simanis, V. (2004). SIN and the art of splitting the fission yeast cell. *Curr. Biol.* **14**, R722-R730.

Kuntz, K. and O'Connell, M. J. (2009). The G(2) DNA damage checkpoint: could this ancient regulator be the Achilles heel of cancer? *Cancer Biol. Ther.* **8**, 1433-1439.

Lehmann, A., Katayama, S., Harrison, C., Dhut, S., Kitamura, K., McDonald, N. and Toda, T. (2004). Molecular interactions of fission yeast Skp1 and its role in the DNA damage checkpoint. *Genes Cells* **9**, 367-382.

Lindqvist, A., Rodríguez-Bravo, V. and Medema, R. H. (2009). The decision to enter mitosis: feedback and redundancy in the mitotic entry network. *J. Cell Biol.* **185**, 193-202.

López-Avilés, S., Grande, M., González, M., Helgesen, A. L., Alemany, V., Sanchez-Piris, M., Bachs, O., Millar, J. B. and Aligue, R. (2005). Inactivation of the Cdc25 phosphatase by the stress-activated Srk1 kinase in fission yeast. *Mol. Cell* **17**, 49-59.

Lundgren, K., Walworth, N., Booher, R., Dembski, M., Kirschner, M. and Beach, D. (1991). mik1 and wee1 cooperate in the inhibitory tyrosine phosphorylation of cdc2. *Cell* **64**, 1111-1122.

Martin, S. G. and Berthelot-Grosjean, M. (2009). Polar gradients of the DYRK-family kinase Pom1 couple cell length with the cell cycle. *Nature* **459**, 852-856.

Matthews, J. C., Hori, K. and Cormier, M. J. (1977). Purification and properties of Renilla reniformis luciferase. *Biochemistry* **16**, 85-91.

McGowan, C. H. and Russell, P. (1995). Cell cycle regulation of human WEE1. *EMBO J.* **14**, 2166-2175.

Michael, W. M. and Newport, J. (1998). Coupling of mitosis to the completion of S phase through Cdc34-mediated degradation of Wee1. *Science* **282**, 1886-1889.

Millar, J. B., McGowan, C. H., Lenaers, G., Jones, R. and Russell, P. (1991). p80cdc25 mitotic inducer is the tyrosine phosphatase that activates p34cdc2 kinase in fission yeast. *EMBO J.* **10**, 4301-4309.

Millar, J. B., Buck, V. and Wilkinson, M. G. (1995). Pyp1 and Pyp2 PTPases dephosphorylate an osmosensing MAP kinase controlling cell size at division in fission yeast. *Genes Dev.* **9**, 2117-2130.

Mishra, M., Karagiannis, J., Trautmann, S., Wang, H., McCollum, D. and Balasubramanian, M. K. (2004). The Clp1p/Flp1p phosphatase ensures completion of cytokinesis in response to minor perturbation of the cell division machinery in Schizosaccharomyces pombe. *J. Cell Sci.* **117**, 3897-3910.

Mitchison, J. M. and Nurse, P. (1985). Growth in cell length in the fission yeast Schizosaccharomyces pombe. *J. Cell Sci.* **75**, 357-376.

Mocciaro, A. and Schiebel, E. (2010). Cdc14: a highly conserved family of phosphatases with non-conserved functions? *J. Cell Sci.* **123**, 2867-2876.

Moreno, S., Klar, A. and Nurse, P. (1991). Molecular genetic analysis of fission yeast Schizosaccharomyces pombe. *Methods Enzymol.* **194**, 795-823.

Morgan, D. O. (1997). Cyclin-dependent kinases: engines, clocks, and microprocessors. *Annu. Rev. Cell Dev. Biol.* **13**, 261-291.

Moseley, J. B. and Nurse, P. (2009). Cdk1 and cell morphology: connections and directions. *Curr. Opin. Cell Biol.* **21**, 82-88.

Moseley, J. B., Mayeux, A., Paoletti, A. and Nurse, P. (2009). A spatial gradient coordinates cell size and mitotic entry in fission yeast. *Nature* **459**, 857-860.

Nalepa, G. and Harper, J. W. (2004). Visualization of a highly organized intranuclear network of filaments in living mammalian cells. *Cell Motil. Cytoskeleton* **59**, 94-108.

Nilsson, I. and Hoffmann, I. (2000). Cell cycle regulation by the Cdc25 phosphatase family. *Prog. Cell Cycle Res.* **4**, 107-114.

Núñez, A., Franco, A., Soto, T., Vicente, J., Gacto, M. and Cansado, J. (2010). Fission yeast receptor of activated C kinase (RACK1) ortholog Cpc2 regulates mitotic commitment through Wee1 kinase. *J. Biol. Chem.* **285**, 41366-41373.

Nurse, P. (1990). Universal control mechanism regulating onset of M-phase. *Nature* **344**, 503-508.

Nurse, P. (1994). Ordering S phase and M phase in the cell cycle. *Cell* **79**, 547-550.

O'Connell, M. J., Raleigh, J. M., Verkade, H. M. and Nurse, P. (1997). Chk1 is a wee1 kinase in the G2 DNA damage checkpoint inhibiting cdc2 by Y15 phosphorylation. *EMBO J.* **16**, 545-554.

O'Connell, M. J., Walworth, N. C. and Carr, A. M. (2000). The G2-phase DNA-damage checkpoint. *Trends Cell Biol.* **10**, 296-303.

Petersen, J. and Hagan, I. M. (2005). Polo kinase links the stress pathway to cell cycle control and tip growth in fission yeast. *Nature* **435**, 507-512.

Petersen, J. and Nurse, P. (2007). TOR signalling regulates mitotic commitment through the stress MAP kinase pathway and the Polo and Cdc2 kinases. *Nat. Cell Biol.* **9**, 1263-1272.

Raleigh, J. M. and O'Connell, M. J. (2000). The G(2) DNA damage checkpoint targets both Wee1 and Cdc25. *J. Cell Sci.* **113**, 1727-1736.

Rhind, N. and Russell, P. (2001). Roles of the mitotic inhibitors Wee1 and Mik1 in the G(2) DNA damage and replication checkpoints. *Mol. Cell. Biol.* **21**, 1499-1508.

Rhind, N., Furnari, B. and Russell, P. (1997). Cdc2 tyrosine phosphorylation is required for the DNA damage checkpoint in fission yeast. *Genes Dev.* **11**, 504-511.

Russell, P. and Nurse, P. (1986). cdc25+ functions as an inducer in the mitotic control of fission yeast. *Cell* **45**, 145-153.

Russell, P. and Nurse, P. (1987a). The mitotic inducer nim1+ functions in a regulatory network of protein kinase homologs controlling the initiation of mitosis. *Cell* **49**, 569-576.

Russell, P. and Nurse, P. (1987b). Negative regulation of mitosis by wee1+, a gene encoding a protein kinase homolog. *Cell* **49**, 559-567.

Seeger, M., Gordon, C., Ferrell, K. and Dubiel, W. (1996). Characteristics of 26 S proteases from fission yeast mutants, which arrest in mitosis. *J. Mol. Biol.* **263**, 423-431.

Shiozaki, K., Shiozaki, M. and Russell, P. (1998). Heat stress activates fission yeast Spc1/StyI MAPK by a MEKK-independent mechanism. *Mol. Biol. Cell* **9**, 1339-1349.

Sia, R. A., Bardes, E. S. and Lew, D. J. (1998). Control of Swe1p degradation by the morphogenesis checkpoint. *EMBO J.* **17**, 6678-6688.

Stegmeier, F. and Amon, A. (2004). Closing mitosis: the functions of the Cdc14 phosphatase and its regulation. *Annu. Rev. Genet.* **38**, 203-232.

Suda, M., Yamada, S., Toda, T., Miyakawa, T. and Hirata, D. (2000). Regulation of Wee1 kinase in response to protein synthesis inhibition. *FEBS Lett.* **486**, 305-309.

Tallada, V. A., Bridge, A. J., Emery, P. A. and Hagan, I. M. (2007). Suppression of the Schizosaccharomyces pombe cut12.1 cell-cycle defect by mutations in cdc25 and genes involved in transcriptional and translational control. *Genetics* **176**, 73-83.

Trautmann, S., Wolfe, B. A., Jorgensen, P., Tyers, M., Gould, K. L. and McCollum, D. (2001). Fission yeast Clp1p phosphatase regulates G2/M transition and coordination of cytokinesis with cell cycle progression. *Curr. Biol.* **11**, 931-940.

Journal of Cell Science

Ubersax, J. A., Woodbury, E. L., Quang, P. N., Paraz, M., Blethrow, J. D., Shah, K., Shokat, K. M. and Morgan, D. O. (2003). Targets of the cyclin-dependent kinase Cdk1. *Nature* **425**, 859-864.

Vassilev, L. T., Tovar, C., Chen, S., Knezevic, D., Zhao, X., Sun, H., Heimbrook, D. C. and Chen, L. (2006). Selective small-molecule inhibitor reveals critical mitotic functions of human CDK1. *Proc. Natl. Acad. Sci. USA* **103**, 10660-10665.

VerPlank, L. and Li, R. (2005). Cell cycle-regulated trafficking of Chs2 controls actomyosin ring stability during cytokinesis. *Mol. Biol. Cell* **16**, 2529-2543.

Wang, H., Zhou, N., Ding, F., Li, Z., Chen, R., Han, A. and Liu, R. (2011). An efficient approach for site-directed mutagenesis using central overlapping primers. *Anal. Biochem.* **418**, 304-306.

Wang, Y., Li, W. Z., Johnson, A. E., Luo, Z. Q., Sun, X. L., Feoktistova, A., McDonald, W. H., McLeod, I., Yates, J. R., 3rd, Gould, K. L. et al. (2012). Dnt1 acts as a mitotic inhibitor of the spindle checkpoint protein dma1 in fission yeast. *Mol. Biol. Cell* **23**, 3348-3356.

Watanabe, N., Arai, H., Nishihara, Y., Taniguchi, M., Watanabe, N., Hunter, T. and Osada, H. (2004). M-phase kinases induce phospho-dependent ubiquitination of somatic Wee1 by SCFbeta-TrCP. *Proc. Natl. Acad. Sci. USA* **101**, 4419-4424.

Watanabe, N., Arai, H., Iwasaki, J., Shiina, M., Ogata, K., Hunter, T. and Osada, H. (2005). Cyclin-dependent kinase (CDK) phosphorylation destabilizes somatic Wee1 via multiple pathways. *Proc. Natl. Acad. Sci. USA* **102**, 11663-11668.

Wolfe, B. A. and Gould, K. L. (2004). Fission yeast Clp1p phosphatase affects G2/M transition and mitotic exit through Cdc25p inactivation. *EMBO J.* **23**, 919-929.

Wolfe, B. A., McDonald, W. H., Yates, J. R., 3rd and Gould, K. L. (2006). Phospho-regulation of the Cdc14/Clp1 phosphatase delays late mitotic events in S. pombe. *Dev. Cell* **11**, 423-430.

Yamano, H., Gannon, J. and Hunt, T. (1996). The role of proteolysis in cell cycle progression in Schizosaccharomyces pombe. *EMBO J.* **15**, 5268-5279.

Fig. S1. The rescuing effect of *dnt1Δ* on temperature-sensitive SIN mutant *sid2-250* and actomyosin ring formation mutant *cdc8-110* is reversed by higher level of Cdc25 induced by gain-of-function version of *cdc25*$^{+}$ (*cdc25-D1*). Serial dilutions (10-fold) of the indicated strains were spotted on EMM plus or without thiamine after being grown in YE and then washed by EMM liquid and incubated for 3–5 days at the indicated temperatures before being photographed.

Fig. S2. Quantification of cell lengths at cell division in double mutants between *dnt1Δ* and known cell cycle regulator mutants. Cells were grown in EMM at 25°C and n>200 cells with septa were measured for each genotype. Data are presented as in Fig. 1E. ***P<0.001.

Fig. S3. Dnt1 regulates G2/M transition independently of G2 DNA damage checkpoint and RACK1 kinase Cpc2. (A) Quantification of cell lengths at cell division in double mutants between *dnt1Δ* and G2 DNA damage checkpoint mutants. Cells were grown in EMM at 25°C and n>200 cells with septa were measured for each genotype. ***P<0.001. (B) Quantification of cell lengths at cell division in double mutants between *dnt1Δ* and *cpc2Δ* mutant. Cells were grown in EMM at 30°C and n>200 cells with septa were measured for each genotype. ***P<0.001. (C) *cpc2Δ* further enhanced the rescue of SIN mutant *cdc14-118* by *dnt1Δ*, showing additive effect. Serial dilutions (10-fold) of the indicated strains were performed as described in Fig. 1B.

Fig. S4. Cut12 and Dma1 are not involved in Dnt1 regulation of G2/M transition. (A) Quantification of cell lengths at cell division in double mutants between *dnt1Δ* and *dma1Δ* or *cut12-S11*. Cells were grown in YE at 25°C and n>200 cells with septa were measured for each genotype. ***P<0.001. **P<0.01. (B) Negative genetic interaction between *dnt1Δ* and *cdc25-22* cannot be rescued by *dma1Δ* or gain-of-function mutant *cut12-S11*. Serial dilutions (10-fold) of the indicated strains were spotted on YE plates and incubated for 3–5 days at the indicated temperatures before being photographed.

Fig. S5. Protein levels of other Cdk1 regulators, such as Cdc25, Cdc13 (cyclin B) or Cdr2 are not altered in *dnt1Δ* mutant. Protein samples were prepared from wild type and *dnt1Δ* strains with or without *cdc25-12myc*, *cdc13-HA* or *cdr2-2HA-6His*. Immunoblotting was performed with anti-myc or anti-HA antibodies depending the tagged proteins to be detected. The levels of each Cdk1 regulator protein were normalized to those of total Cdc2 in each strain. n=3. P>0.05.

Fig. S6. *wee1Δ* completely abolished rescuing capability of *dnt1Δ* on actomyosin ring formation mutant *cdc8-110*. (A) Serial dilutions (10-fold) of the indicated strains were spotted on YE plates and incubated for 3–5 days at the indicated temperatures before being photographed. (B) The frequencies of cells with multiple nuclei (as indication of cytokinetic defects) were quantified in single, double and triple mutants with indicated genotypes, as described in Fig. 4C.

Fig. S7. Dma1 and Cut12 are not involved in SIN regulation by Dnt1. (A and B) Deletion of *dma1*$^{+}$ does not affect the rescue of SIN mutant *cdc14-118* by *dnt1Δ*. (A) Serial dilutions (10-fold) of the indicated strains were spotted on YE plates and incubated for 3–5 days at the indicated temperatures before being photographed. (B) The frequencies of cells with multiple nuclei (as indication of cytokinetic defects) were quantified in single, double and triple mutants with indicated genotypes, as described in Fig. 4C. (C and D) The gain-of-function mutant *cut12-S11* does not affect the rescue of SIN mutant *cdc14-118* by *dnt1Δ*. Drop test of serial dilutions and quantification of multiple nuclei were analyzed as for *dma1Δ* mutants in A and B.

Table S1. Yeast strains used in this study.

Yu et al., Supplementary Figure S1.

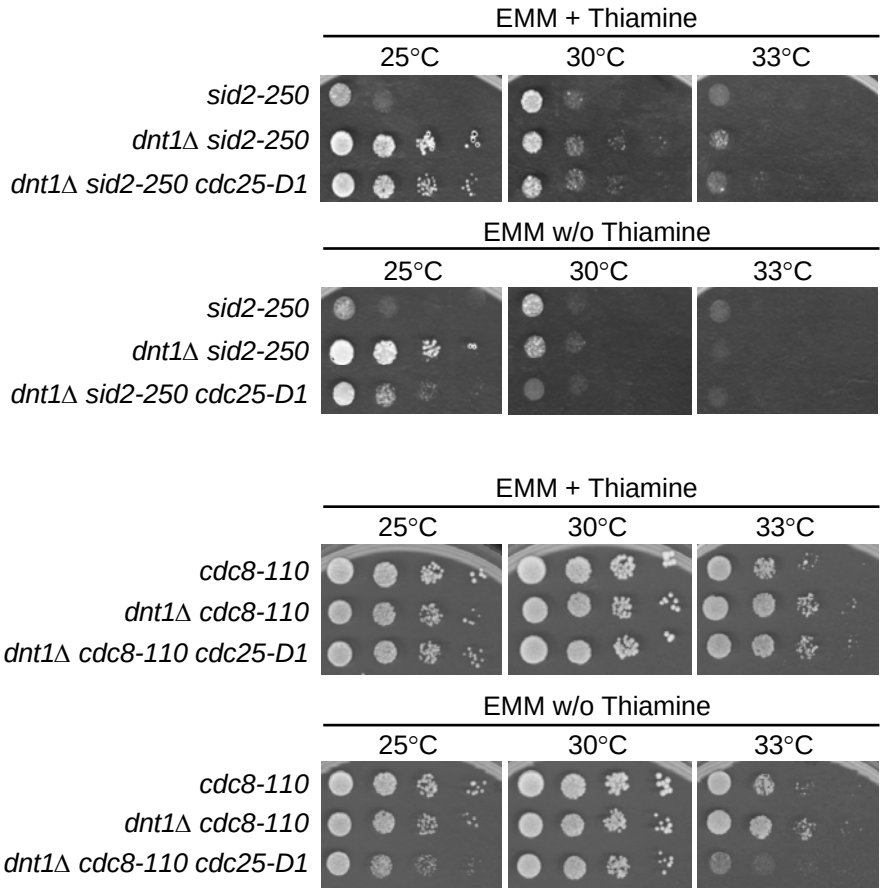

Yu et al., Supplementary Figure S2.

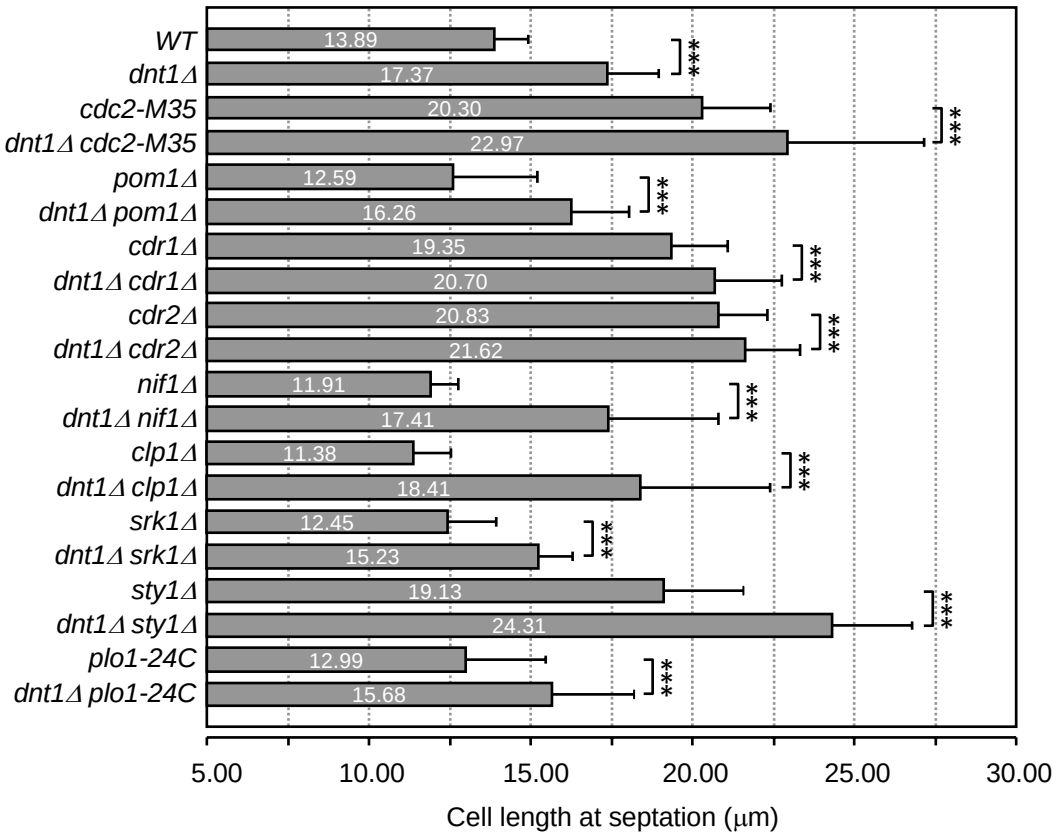

Yu et al., Supplementary Figure S3.

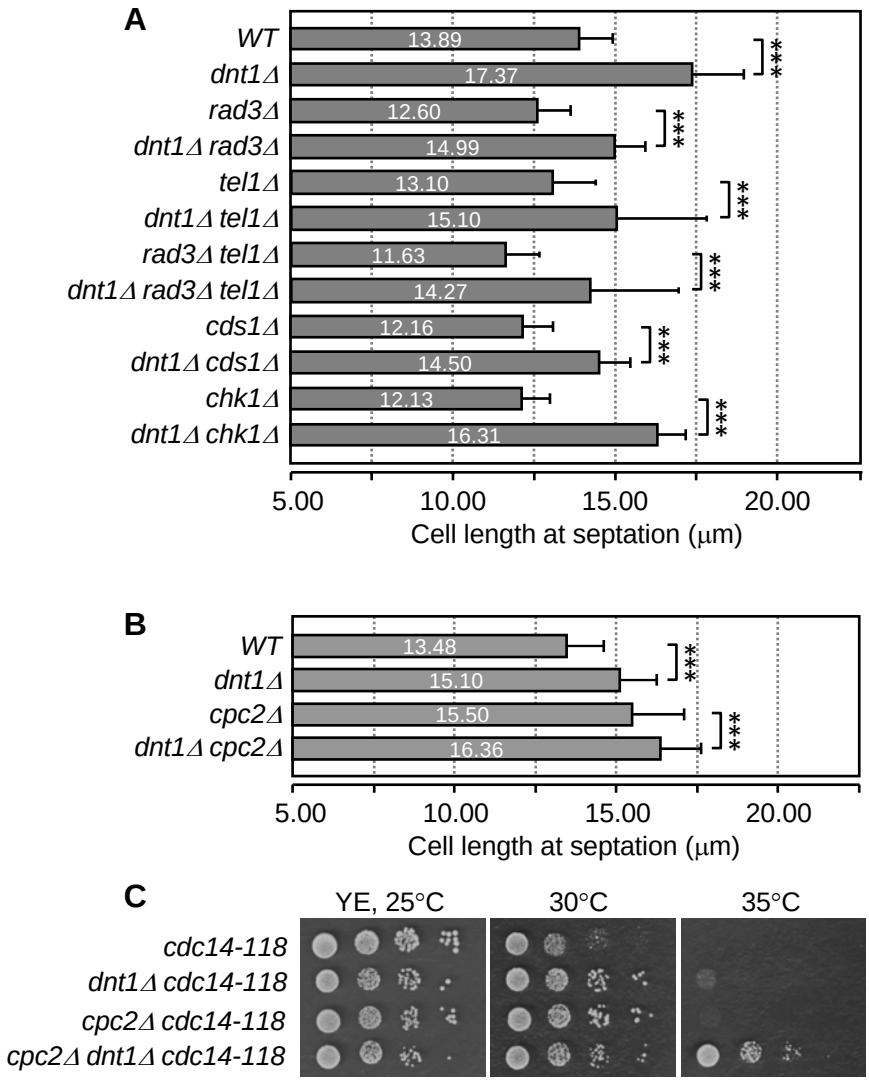

Yu et al., Supplementary Figure S4.

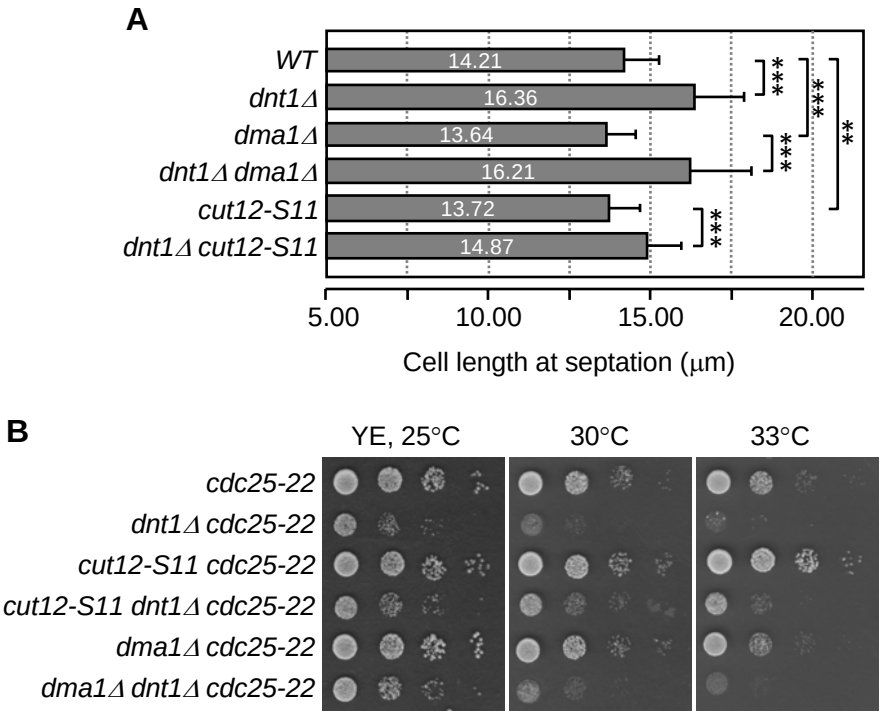

Yu et al., Supplementary Figure S5.

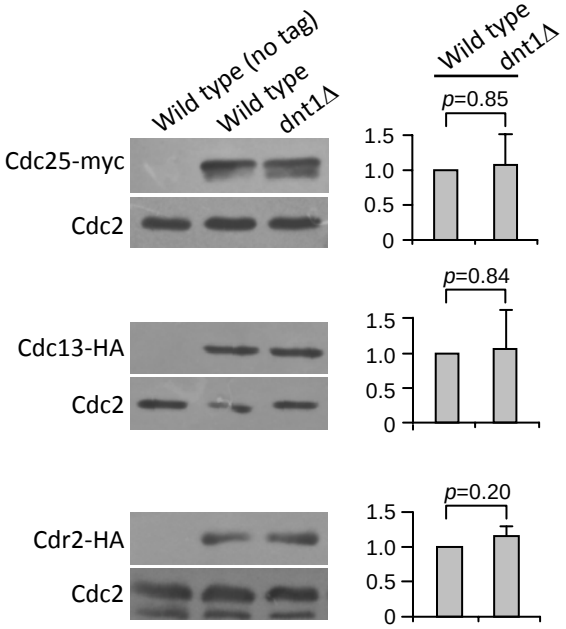

Yu et al., Supplementary Figure S6.

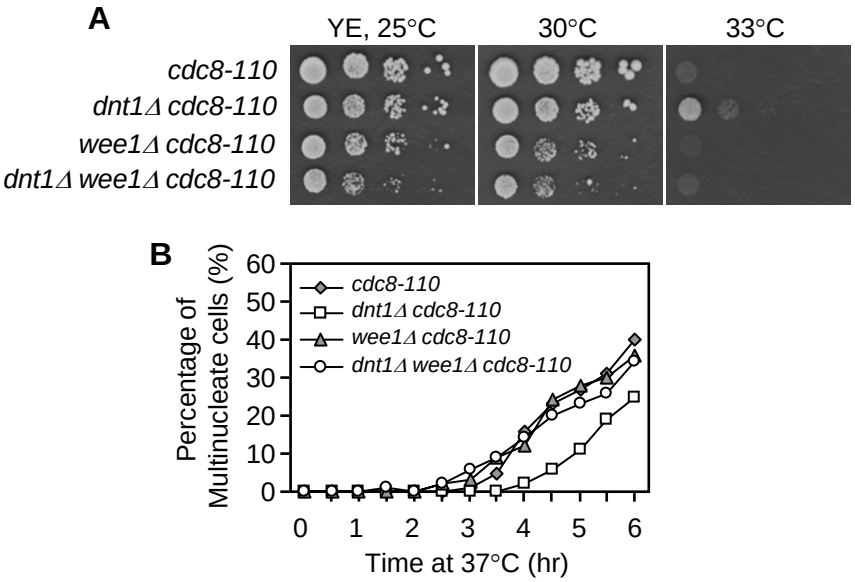

Yu et al., Supplementary Figure S7.

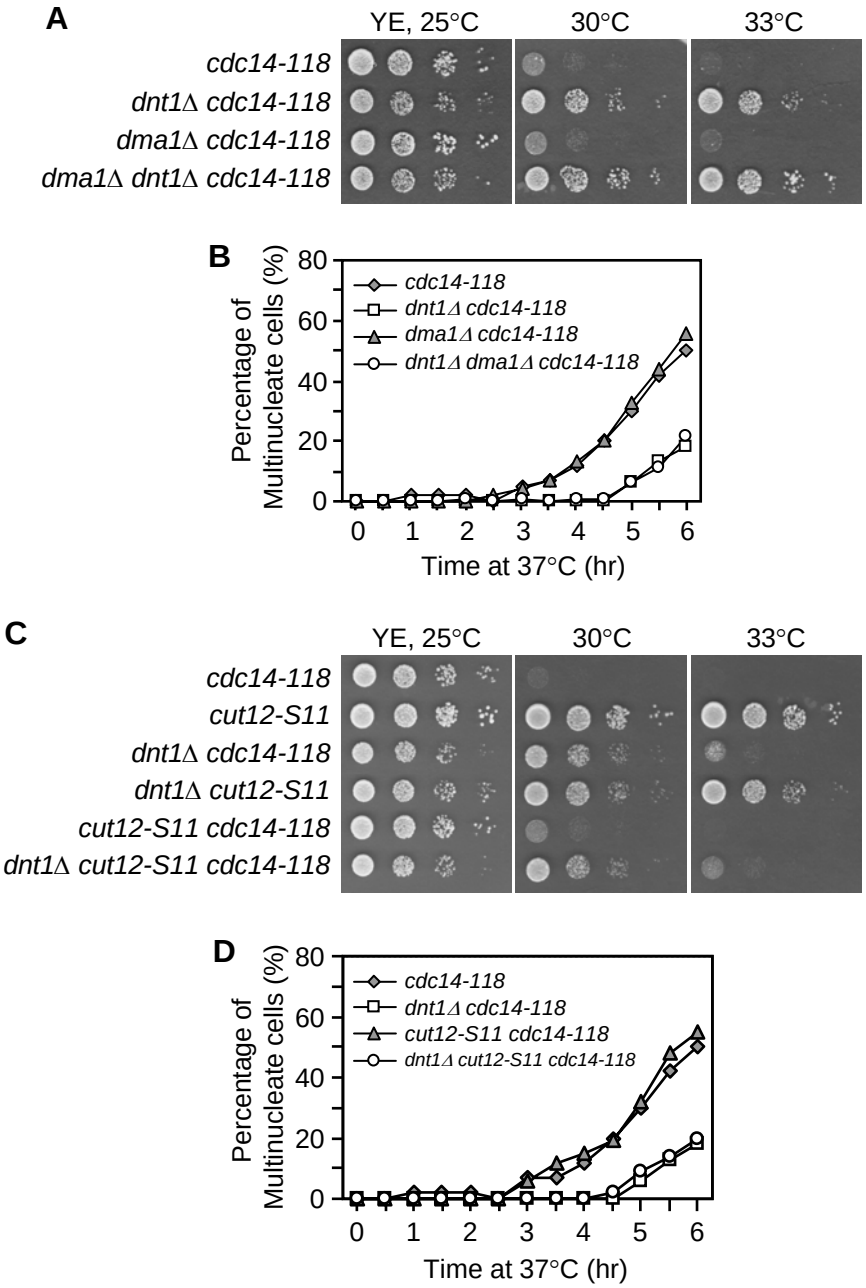

Table S1. Yeast strains used in this study

Strain Name	Genotype
JY1	*h⁻ leu1-32 ura4-D18 ade6-210*
JY2	*h⁺ leu1-32 ura4-D18 ade6-210*
JY109	*h⁻ dnt1Δ::ura4⁺ ade6-210 leu1-32 ura4-D18*
JY145	*h⁺ dnt1Δ::kanR ade6-210 leu1-32 ura4-D18*
JY2166	*h⁹⁰ cdc2-M35 ura4-D18 leu1-32*
JY2281	*h? dnt1Δ::ura4⁺ cdc2-M35 ura4-D18 leu1-32*
JY2423	*h⁺ cdr1Δ::kanR his2 leu1-32 ura4-D18*
JY2470	*h? dnt1Δ::ura4⁺ cdr1Δ::kanR his2 leu1-32 ura4-D18*
JY 2155	*h⁻ cdr2Δ::ura4⁺ ura4-D18*
JY 2204	*h? dnt1Δ::kanR cdr2Δ::ura4⁺ ura4-D18*
JY 2159	*h⁻ cmk2Δ::ura4⁺ ura4-D18*
JY 2278	*h? dnt1Δ::kanR cmk2Δ::ura4⁺ ura4-D18*
JY 2165	*h⁻ cdc2-1w leu1*
JY 2229	*h? dnt1Δ::kanR cdc2-1w leu1*
JY 2137	*h⁺ cpc2Δ::kanR ade⁻ leu⁻ ura⁻*
JY 2194	*h⁺ cpc2Δ::kanR dnt1Δ::ura4⁺ ade⁻ leu⁻ ura⁻*
JY125	*h⁻ dnt1-13myc::kanR ade6-210 leu1-32 ura4-D18*
JY2136	*h⁺ cpc2-GFP::kanR ade⁻ leu⁻ ura⁻*
JY2493	*h? dnt1-13myc::kanR cpc2-GFP::kanR ade⁻ leu⁻ ura⁻*
JY2263	*h? cpc2-GFP::kanR dnt1Δ::ura4⁺ ade⁻ leu⁻ ura⁻*
JY2357	*h⁻ nif1Δ::ura4⁺ ura4-D18*
JY2409	*h? dnt1Δ::kanR nif1Δ::ura4⁺ ura4-D18*
JY18	*h⁻ wee1-50 ade6-21x his3-D1 leu1-32 ura4-D18*
JY2395	*h? dnt1Δ::kanR wee1-50 ade6-21x his3-D1 leu1-32 ura4-D18*
JY2558	*h⁺ wee1-50 mik1Δ::ura4⁺ leu1-32 ura4-D18*
JY2562	*h? dnt1Δ::kanR wee1-50 mik1Δ::ura4⁺ leu1-32 ura4-D18*
JY2160	*h⁻ srk1Δ::ura4⁺ ura4-D18*
JY2267	*h? dnt1Δ::kanR srk1Δ::ura4⁺ ura4-D18*
JY2162	*h⁻ sty1Δ::ura4⁺*
JY2333	*h? dnt1Δ::kanR sty1Δ::ura4⁺ ura4-D18*
JY14	*h⁻ plo1-24C ade6-210 leu1-32 ura4-D18*
JY439	*h⁻ dnt1Δ::kanR plo1-24C ade6-21x leu1-32 ura4-D18*
JY492	*h⁻ pom1Δ::ura4⁺ leu⁻ ura⁻*

JY2084	*h? dnt1Δ::kanR pom1Δ::ura4+ leu- ura-*
JY1694	*h+ dnt1Δ::ura4+ cdc8-110 leu1-32 ura4-D18*
JY1849	*h? dnt1Δ::kanR cdc8-110 leu1-32::P_{nmt1}-cdc25-D1::leu1+ ura4-D18*
JY2758	*h? dnt1Δ::kanR wee1Δ::ura4+ cdc8-110 ura4-D18*
JY2869	*h+ cdc8-110 wee1Δ::ura4+ ura4-D18*
JY47	*h+ cdc14-118 ade6-210 leu1-32 ura4-D18*
JY2211	*h? cdc14-118 leu1-32::P_{nmt1}-cdc25-D1::leu1+ ade6-21x ura4-D18*
JY2212	*h? cdc14-118 leu1-32::P_{nmt1}-cdc25-D1::leu1+ ura4-D18*
JY1110	*h- dnt1Δ::kanR cdc14-118 ade6-210 ura4-D18*
JY2177	*h? dnt1Δ::kanR cdc14-118 leu1-32::P_{nmt1}-cdc25-D1::leu1+ ade6-210 ura4-D18*
JY2867	*h? wee1Δ::ura4+ cdc14-118 ura4-D18*
JY2441	*h? cpc2Δ::kanR cdc14-118 ade- leu- ura-*
JY2504	*h? cpc2Δ::kanR dnt1Δ::ura4+ cdc14-118 ade- leu- ura-*
JY2662	*h- wee1-3HA6H leu1-32 ura4-D18*
JY2715	*h? dnt1Δ::ura4+ wee1-3HA6H leu1-32 ura4-D18*
JY22	*h+ cdc25-22 ura4-D18*
JY1845	*h? dnt1Δ::kanR cdc25-22 ura4-D18*
JY7	*h- cdc8-110 leu1-32 his3-D1 ura4-D18*
JY2361	*h- cdr2-2HA-6His::ura4+ leu1-32 ura4-D18*
JY2412	*h? dnt1Δ::kanR cdr2-2HA-6His::ura4+ leu1-32 ura4-D18*
JY270	*h- cdc13-HA::ura4+ leu1 ura4-D18*
JY1836	*h? dnt1Δ::kanR cdc13-HA::ura4+ leu1-32 ura4-D18*
JY2156	*h- wee1Δ::ura4+*
JY2270	*h? dnt1Δ::kanR wee1Δ::ura4+ ura4-D18*
JY1652	*h- leu1-32::P_{nmt1}-cdc25-D1::leu1+ ura-*
JY1800	*h- dnt1Δ::kanR leu1-32::P_{nmt1}-cdc25-D1::leu1+ ade6-210 ura4-D18*
JY61	*h+ clp1Δ::ura4+ ade6-216 leu1-32 ura4-D18*
JY130	*h- dnt1Δ::ura4+ clp1Δ::ura4+ ade6-21x leu1-32 ura4-D18*
JY2943	*h- rad3Δ::ura4+ leu1-32 ura4-D18*
JY2984	*h+ dnt1Δ::kanR rad3Δ::ura4+ leu1-32 ura4-D18*
JY2947	*h- chk1Δ::ura4+ ade6-704 leu1-32 ura4-D18*
JY2991	*h+ dnt1Δ::kanR chk1Δ::ura4+ leu1-32 ura4-D18*
JY2944	*h- cds1Δ::ura4+ leu1-32 ura4-D18*
JY2993	*h- dnt1Δ::kanR cds1Δ::ura4+ leu1-32 ura4-D18*
JY2163	*h- cdc2-3w cdc25Δ::ura4+ leu1-32 ura4-D18*
JY2327	*h+ dnt1Δ::kanR cdc2-3w ade6-21x ura4-D18*

JY1693	*h⁻ cdc25-12myc::ura4⁺ leu1-32 ura4-D18*
JY1744	*h? dnt1Δ::kanR cdc25-12myc::ura4⁺ leu1-32 ura4-D18*
JY44	*h⁺ sid2-250 ade6-21x leu1-32 ura4-D18*
JY2576	*h⁺ dnt1Δ::ura4⁺ sid2-250 ade6-21x leu1-32 ura4-D18*
JY3047	*h? wee1Δ::ura4⁺ sid2-250 ura4-D18*
JY3049	*h? dnt1Δ::kanR wee1Δ::ura4⁺ sid2-250 ura4-D18*
JY2762	*h? dnt1Δ::kanR sid2-250 ade6-21x leu1-32 ura4-D18*
JY2765	*h? sid2-250 leu1-32::P_{nmt1}-cdc25-D1::leu1⁺ ade6-21x ura4-D18*
JY3507	*h⁻ ade4-luc::kanR wee1-R.luc::natR leu1-32 ura4-18*
JY3583	*h⁺ dnt1Δ::ura4⁺ ade4-luc::kanR wee1-R.luc::natR leu1-32 ura4-D18*
JY3576	*h⁺ mts3-1 ade4-luc::kanR wee1-R.luc::natR leu1-32 ura4-D18*
JY3626	*h⁺ skp1-A7 ade4-luc::kanR wee1-R.luc::natR leu1 ura4*
JY3640	*h⁻ dnt1Δ::ura4⁺ skp1-A7 ade4-luc::kanR wee1-R.luc::natR leu1 ura4*
JY3514	*h⁺ tel1Δ::LEU2⁺ ade6-210 leu1-32 ura4-D18*
JY3595	*h⁺ dnt1Δ::kanR tel1Δ::LEU2⁺ ade6-210 leu1-32 ura4-D18*
JY3597	*h⁻ dnt1Δ::kanR rad3Δ::ura4⁺ tel1Δ::LEU2⁺ ade6-210 leu1-32 ura4-D18*
JY3649	*h⁻ rad3Δ::ura4⁺ tel1Δ::LEU2⁺ leu1-32 ura4-D18*
JY3269	*h⁻ skp1-A7 leu1 ura4*
JY3418	*h⁺ dnt1Δ::kanR skp1-A7 leu1 ura4*
JY3480	*h⁻ skp1-A7 cdc14-118 leu1 ura4*
JY3482	*h⁺ dnt1Δ::kanR skp1-A7 cdc14-118 leu1 ura4*
JY2580	*h? dma1Δ::ura4⁺ cdc14-118 leu1-32 ura4-D18*
JY2582	*h? dma1Δ::ura4⁺ dnt1Δ::kanR cdc14-118 leu1-32 ura4-D18*
JY2499	*h⁺ kanR::P_{81nmt1}-GFP-wee1*
JY4328	*h⁻ kanR::P_{81nmt1}-GFP-wee1 cdc14-118*
JY2312	*h⁺ cut12-S11 leu1-32*
JY2125	*h⁻ dnt1Δ::kanR cut12-S11 leu1-32*
JY2594	*h⁺ cut12-S11 cdc25-22 ade6-210 leu1-32 ura4-D18*
JY2589	*h⁺ dnt1Δ::kanR cdc25-22 cut12-S11 leu1-32 ura4-D18*
JY2595	*h? dnt1Δ::kanR dma1Δ::ura4⁺ cdc25-22 leu1-32 ura4-D18*
JY2596	*h? dma1Δ::ura4⁺ cdc25-22 leu1-32 ura4-D18*
JY4364	*h⁻ cut12-S11 cdc14-118 ade6-21x leu1-32 ura4⁻*
JY4365	*h⁺ dnt1Δ::kanR cut12-S11 cdc14-118 ade6-21x leu1-32*